DNA Nanotechnology as an Emerging Tool to Study Mechanotransduction in Living Systems

Victor Pui-Yan Ma and Khalid Salaita*

The ease of tailoring DNA nanostructures with sub-nanometer precision has enabled new and exciting in vivo applications in the areas of chemical sensing, imaging, and gene regulation. A new emerging paradigm in the field is that DNA nanostructures can be engineered to study molecular mechanics. This new development has transformed the repertoire of capabilities enabled by DNA to include detection of molecular forces in living cells and elucidating the fundamental mechanisms of mechanotransduction. This Review first describes fundamental aspects of force-induced melting of DNA hairpins and duplexes. This is then followed by a survey of the currently available force sensing DNA probes and different fluorescence-based force readout modes. Throughout the Review, applications of these probes in studying immune receptor signaling, including the T cell receptor and B cell receptor, as well as Notch and integrin signaling, are discussed.

1. Introduction

It is widely recognized that mechanical forces underpin many of the molecular processes that maintain life. For example, protein cargo transport, translation, and transcription require spatially and temporally coordinated forces at the 1–20 pN scale. The roots of this idea that physical forces influence biology were initially conceptualized by the Scottish Zoologist D'Arcy Thompson in his seminal work "On growth and form" more than a century ago (**Figure 1**).[1] This theoretical work generated much interest, but there was little progress in the field for many decades. This is because researchers lacked the technologies to measure the miniscule forces applied by cells, let alone single molecules, which hindered further progress in mechanobiology. A key development occurred in 1980, when

V. P.-Y. Ma, Prof. K. Salaita
Department of Chemistry
Emory University
Atlanta, GA 30322, USA
E-mail: k.salaita@emory.edu
Prof. K. Salaita
Wallace H. Coulter Department of Biomedical Engineering
Emory University and Georgia Institute of Technology
Atlanta, GA 30322, USA
Prof. K. Salaita
Winship Cancer Institute
Emory University
Atlanta, GA 30322, USA

The ORCID identification number(s) for the author(s) of this article can be found under https://doi.org/10.1002/smll.201900961.

Harris et al. discovered that cells deform and "wrinkle" a silicone polymer substrate as observed under light microscopy.[2] This observation led to the development of more quantitative methods such as traction force microscopy (TFM)[3] and micropillar arrays[4] that measure polymer deformations to map cellular traction stresses (stress = force/cross-sectional area and is typically in units of Pa). Particularly, TFM has gained wide adoption by the mechanobiology community because of its ease of use and longstanding history. TFM relies on plating cells onto elastic polymer substrates that are doped with fluorescent particles such that particle displacements can be used to computationally infer the stresses experienced by the polymer film. One issue in TFM is that quantifying substrate deformation is an indirect measurement of receptor forces, and the crosslinked nature of the polymer limits TFM's spatial (≈µm) and force resolution (≈nN). In contrast to TFM, single molecule force spectroscopy (SMFS) methods such as atomic force microscopy (AFM), optical/magnetic tweezer (OT/MT), and biomembrane force probe (BFP) detect pN forces exerted by individual cell surface molecules.[5] These methods are generally used to determine the threshold force that leads to ligand–receptor bond dissociation.[6] In other implementations, single molecule methods can be used to measure the forces transmitted by a cell to its receptor upon engaging of a ligand.[7] While these methods have transformed our understanding of the single molecule biophysics of cell surface receptors, their serial nature—interrogating one molecule at a time—is not compatible with the dynamics of living systems where groups of homo and heteroreceptors are typically engaged to trigger signaling events.

In 2011, we addressed the gap between TFM and single molecule force spectroscopy techniques by developing molecular tension fluorescence microscopy (MTFM) where a chip was coated with probe molecules that generate fluorescence in response to 1–20 pN forces (Figure 1).[8] MTFM probes are comprised of a molecular "spring" flanked by a fluorophore–quencher pair and immobilized onto a surface. Each MTFM probe reports on the pN forces transmitted by an individual receptor molecule. In the first generation MTFM, a 24 mer polyethylene-glycol (PEG) polymer that functioned as the extendible spring was used to infer the magnitude of forces applied by the epidermal growth factor receptor. Subsequently, we and others have engineered several new types of MTFM probes that use PEG,[9] nucleic acids,[10] and a variety of engineered polypeptides[11] or proteins[12] as

**ADVANCED
SCIENCE NEWS**

www.advancedsciencenews.com

NANO · MICRO

small

www.small-journal.com

alternative molecular springs. We recently reviewed the evolution and fundamentals of MTFM probe design.[13] The current review will exclusively focus on DNA-based force probes, as they present significant new capabilities that are rapidly transforming our understanding of mechanobiology (Figure 1).

The role of DNA as a material for storage of genetic information is well documented in the central dogma of biology. The use of nucleic acids as a material that can be engineered to self-assemble into nanostructures started to appear in the early 80s through the seminal work of Seeman.[14] It was proposed and demonstrated that the molecular recognition (base pairing) of nucleic acids could be utilized to build complex structures not found in vivo,[14] and this work subsequently led to the birth of "DNA nanotechnology."[15] At the same period of time, the repertoire of nucleic acid structures and functions has also vastly expanded as exemplified by the discovery of aptamers,[16] which belong to a class of nucleic acids capable of recognizing analytes with affinities rivaling synthetic antibodies,[17] and DNAzymes, which are catalytically active DNA molecules.[18] These exciting discoveries have driven the use of nucleic acids in many technologically innovative applications such as hybridization guided programmable colloidal assembly,[19] synthetic motors and walkers,[20] gene regulation,[21] and bioanalytical sensing.[22] Of notable work that is highly relevant to the topic of this review is the early literature by Gaub and co-workers[23] and Crooks and co-workers[24] that used the mechanical properties of DNA duplexes as a reference to measure the relative strength of DNA bonds and for analyte sensing.

The purpose of this review is to highlight the development of DNA-based molecular sensors for live cell force sensing—a nascent but rapidly growing area of research since the inception of the DNA-based MTFM probe in 2013 (Figure 1). We first provide a brief overview of methods that are routinely used to study the mechanical properties of nucleic acids. Next, we discuss the fundamental properties of mechanical melting of DNA duplexes and DNA hairpin secondary structures. We then highlight the achievements in using these DNA-based molecular probes to study forces that are important to cellular functions such as immune cell response, platelet activation, and cell adhesion. Lastly, we conclude this review with a perspective of how to improve the performance of these DNA-based molecular tension probes for sensing forces generated by live cells.

2. Methods to Characterize the Mechanical Properties of Nucleic Acid Structures

There is a well-established literature that characterizes the mechanical properties of DNA nanostructures because of their prevalence in many essential biological processes.[25] Nucleic acids generally fold into secondary and higher order structures which are disrupted during transcription or translation.[26] Enzymes such as DNA primase,[27] helicase,[28] and polymerases[29] act on these nucleic acid structures and generate mechanical forces, allowing for efficient site-controlled biological processes, and justifying the extensive work studying nucleic acid biomechanics.

Victor Pui-Yan Ma completed his B.S. degree in chemistry at Hong Kong Baptist University in 2012 and is currently a sixth-year graduate student at Emory University under the supervision of Prof. Khalid Salaita. He is interested in studying mechanoregulation of immune cell signaling using DNA-based force probes.
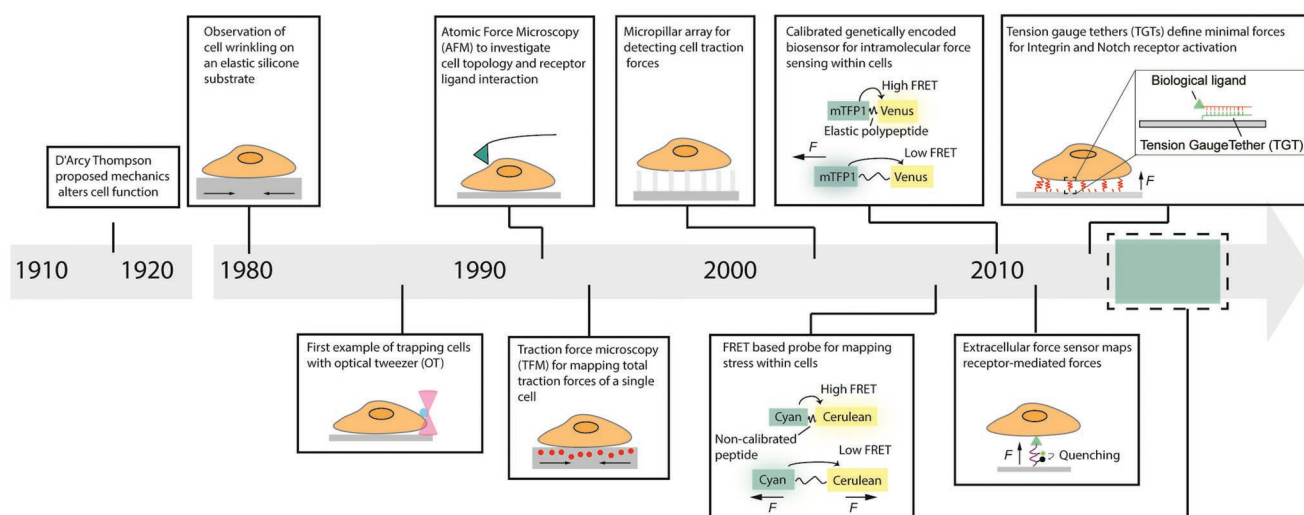
Khalid Salaita received his Ph.D. in chemistry from Northwestern University in 2006 with Prof. Chad A. Mirkin. After a postdoctoral fellowship with Prof. Jay T. Groves at the University of California, Berkeley, he joined Emory University in 2009 where he is currently an Associate Professor of Chemistry. His research group is focused on the interface of nanotechnology and cell biology.

The impact of mechanical force on the energy landscape describing the unfolding trajectory of a protein or nucleic acid is very complex. This energy landscape is time dependent, with folding transitions that are transient in nature and difficult to elucidate experimentally. Recent advances in SMFS methods have started to reveal transition paths and hidden intermediates during mechanical unfolding of biomolecules.[30] For example, one of the most technologically useful ligand–receptor interactions, the biotin–streptavidin bond, was recently investigated using theoretical modeling along with experimental SMFS and showed hidden time-dependent transitions that were previously unknown.[31] Despite this complexity, one way to illustrate the impact of force on biomolecular unfolding is to conceptualize the transition as a 1D, single barrier trajectory, where A and B represent the folded and unfolded state, respectively, separated by an energy barrier of magnitude $\Delta G^{\ddagger}$ (**Figure 2**A).[25] Without the application of force (F), the unfolding is both kinetically and thermodynamically unfavorable due to the high activation barrier ($\Delta G^{\ddagger}$) and higher energy of state B relative to A (ΔG°). F directly modifies the free energy of the molecule by a value proportional to its extension (Δx). Therefore, the reaction rate under F ($k_{\text{forward(F)}}$) is exponentially dependent on the magnitude of F as stated by the Bell model (Equation (1))[32]

$$k_{\text{forward(F)}} = k_0 \exp^{\frac{F\Delta x^{\ddagger}}{k_{\text{b}}T}} \tag{1}$$

ADVANCED
SCIENCE NEWS
www.advancedsciencenews.com

NANO · MICRO
small
www.small-journal.com

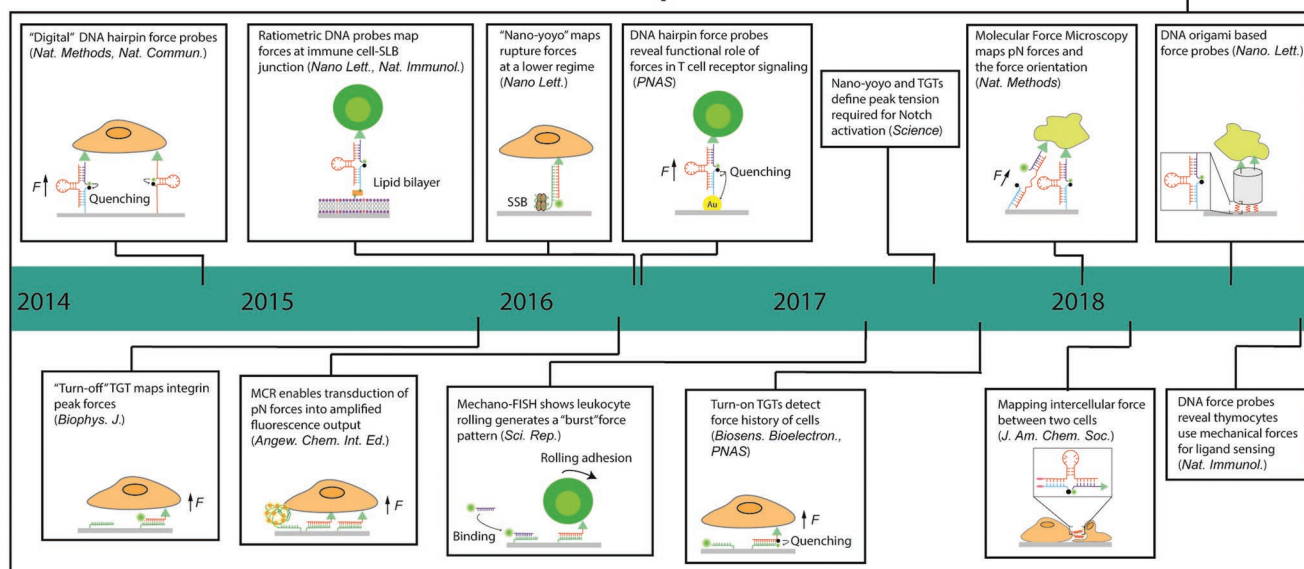## A brief history of cellular biomechanical measurements

Figure 1. Timeline of cellular biomechanical measurements (grey arrow) with a focus on the recent development of DNA-based force sensors (green line).

where $k_{\text{forward(F)}}$ is the rate constant as a function of F, k_0 is the intrinsic rate constant when $F = 0$, $\Delta x^{\ddagger}$ is the distance to the transition state, k_{b} is the Boltzmann constant, and T is temperature.

Our understanding of the mechanical stability of the nucleic acid nanostructures is mostly based on direct measurements using SMFS methods (Figure 2B). In these approaches, one end of the nucleic acid of interest is tethered to a substrate, while the other end is linked to a force transducer such as AFM tip or magnetic bead.[5,33] This can also be achieved using a laser trap system where both ends of the nucleic acids are attached to DNA handles that are tethered to two separate polystyrene beads.[5] Force–extension experiments can be used to measure a specific rupture force of nucleic acids by pulling a construct

at a constant speed (dynamic force spectroscopy).[34] In addition, force clamp experiments can also be used to identify the unfolding force ($F_{1/2}$, which is defined as the force at which the structure has a 50% probability of unfolding) of nucleic acid structures, such as DNA hairpins, where a set of experiments is conducted at different constant forces to record the population of the folded and unfolded states which have different extension lengths. Rupture forces of two-component nucleic acid structures, such as DNA duplexes, can either be acquired from force ramp or force clamp experiments.

Alternatively, hybrid force-fluorescence spectroscopy methods are gaining increasing attention because of their ability to independently reveal both the force–extension relationship and the conformational transitions of the nucleic
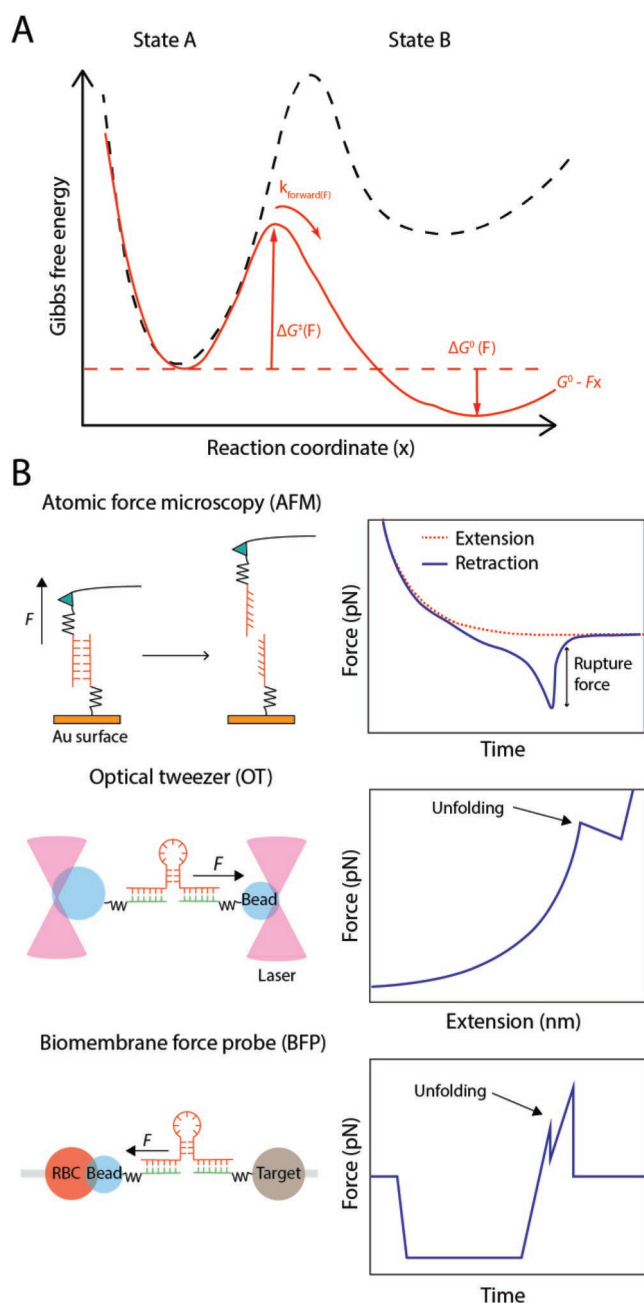
ADVANCED
SCIENCE NEWS
www.advancedsciencenews.com

NANO · MICRO
small
www.small-journal.com

Figure 2. A) Force influences the free energy of a simple two-state thermodynamic system. Red solid curve: with applied force. Dashed black curve: no force. Mechanical force modifies the reaction pathway by lowering the energy of the transition state [$\Delta G^{\ddagger}(F)$], and also the energy of state B. These changes collectively increase the rate for the forward reaction [$k_{forward(F)}$]. B) Single molecule force spectroscopy techniques to measure the mechanical stability of a DNA nanostructure. Idealized force spectra are shown to the right.

acid.[35] These approaches utilize a pair of fluorophores attached to the nucleic acid of interest and rely on single molecule Förster resonance energy transfer (smFRET) as a readout. Coupled with the OT/MT, changes in the smFRET ratios provide a sensitive metric for studying the mechanical stability of nucleic acid nanostructures.

In the following, we aim to highlight the fundamental mechanical properties of the most common DNA structures—DNA hairpins and DNA duplexes. Much of this information was determined from integration of SMFS experiments and computational modeling. These structures are ideally suited as "molecular springs" for performing force measurement with live cells because their unfolding landscapes match the most common force regimes (≈1–50 pN) in mechanotransduction.

2.1. Mechanical Melting of DNA Hairpins

DNA hairpins formed from a single-stranded DNA (ssDNA) consist of an intramolecular base-paired "stem" region and a "loop" region containing unpaired nucleobases. It has been experimentally shown that the structural transition of a hairpin molecule is "digital" and occurs at a very narrow range of applied forces, because the force-induced unfolding of this structure is highly cooperative. For simple hairpin structures with short stem-loop regions, one can assume that they adopt two-state transitions—folded and unfolded states (**Figure 3**A) with an energy difference separated by an activation barrier.[36] The mechanical stability of the hairpin ($F_{1/2}$) is defined by ΔG_{unfold} and $\Delta G_{stretch}$, as shown in Equation (2)

$$F_{1/2} = \frac{(\Delta G_{unfold} + \Delta G_{stretch})}{\Delta x} \tag{2}$$

where $F_{1/2}$ of hairpin is the equilibrium force required to drive hairpin unfolding with 50% probability, ΔG_{fold} is the free energy of DNA hybridization of the hairpin structure at zero force, $\Delta G_{stretch}$ is the free energy to stretch the hairpin structure upon unfolding (Equation (3)), and Δx is the opening distance of hairpin from folded state to unfolded state typically identified from the corresponding force–extension curve, or estimated using the contour length per DNA nucleotide = 0.44 ± 0.02 nm, plus a correction term called the "effective helix width" of 2.0 nm.[36] The $\Delta G_{stretch}$ can be calculated using Equation 3 as follows

$$\Delta G_{stretch} = \left(\frac{k_b T}{L_p}\right)\left[\frac{L_o}{4\left(1 - \frac{x}{L_o}\right)}\right]\left[3\left(\frac{x}{L_o}\right)^2 - 2\left(\frac{x}{L_o}\right)^3\right] \tag{3}$$

where k_b is the Boltzmann constant, T is the temperature, L_p is the persistence length and L_0 is the contour length of ssDNA, x is the hairpin extension from equilibrium.

ΔG_{unfold} is an intrinsic thermodynamic property of folded DNA hairpins dictated by the free energy of collective base-pair stacking and hydrogen bonding. As illustrated in Figure 3B, increasing the guanine–cytosine (GC) content within the stem region of hairpin structures while keeping the stem-length constant increases the ΔG_{unfold} and also the $F_{1/2}$. This is because GC base pairs have higher thermostability than that of adenine and thymine base pairs (more negative ΔG).

Free energy of stretching ($\Delta G_{stretch}$) also has a role in modulating the $F_{1/2}$ of a hairpin. Considering an external force applied to unfold the hairpin, the base pairs in the helix are forced to
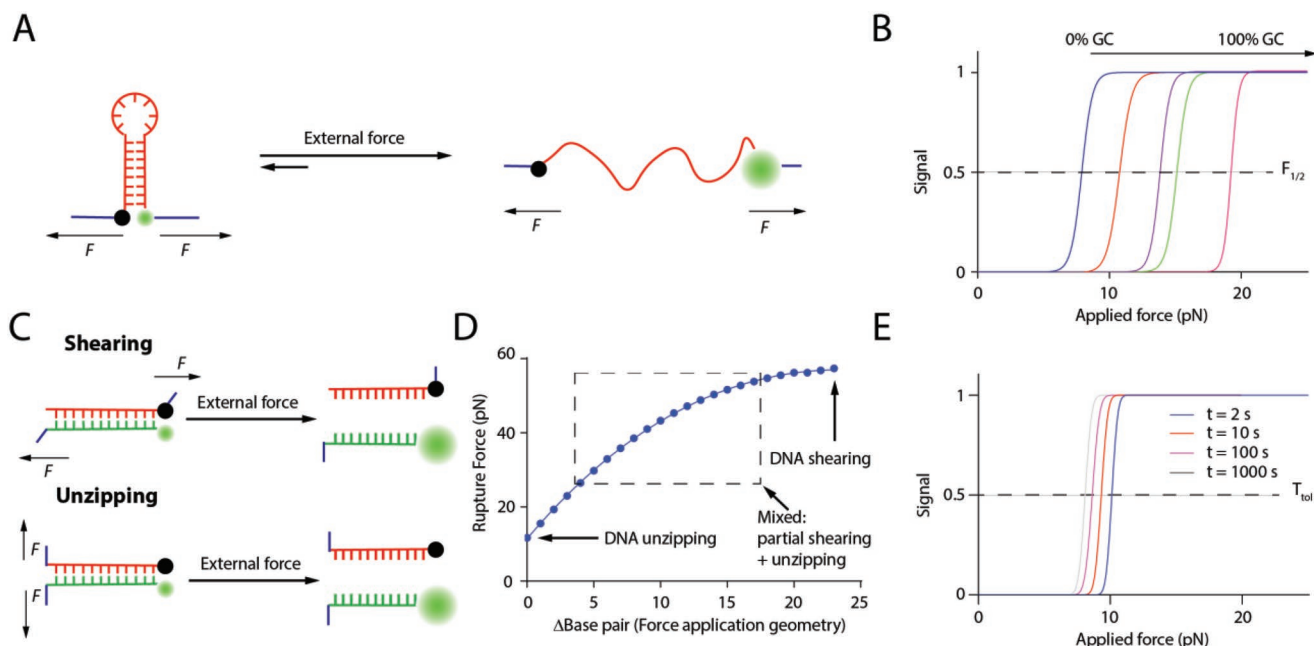
Figure 3. A) Mechanical unfolding of stem-loop region of a DNA-based force probe. B) Theoretical plot showing unfolding of DNA hairpin structures with the same length. Dashed black line indicates 50% expected increase in fluorescence signal at a force defined as $F_{1/2}$. Increasing GC content in the stem-loop structure increases $F_{1/2}$ of the hairpin structure. $F_{1/2}$ data is obtained from optical trap experiment.[36] C) Rupturing of a DNA duplex with different force application geometries. D) Hypothetical plot showing the rupture force of a 24 mer duplex by changing the force application geometry based on the de Gennes DNA rupture model. ΔBase pair is determined by the base pair number between two force anchoring points. The corresponding rupture force is estimated using Equation (4). E) Theoretical plot showing unzipping of a DNA duplex as a function of the applied forces. A threshold force required to attain 50% of the fluorescence signal decreases as the force loading time increases from 2 to 1000 s. Stimulation data obtained.[41]

"unzip" instantaneously producing a ssDNA region. The nucleotides in this region and the loop are mechanically stretched behaving like an "entropic spring". Total extension of this ssDNA region is assumed to follow the worm-like chain (WLC) model, which describes force as a function of the molecular extension of the unfolded hairpin. This means that increasing the stem-loop length of the hairpin has a collective effect in modulating the ΔG_{fold}, as more base pairs can be formed, and the $\Delta G_{stretch}$, which is dictated by the contour length of the hairpin stem-loop. The $F_{1/2}$ of most of the reported hairpins can span from a few pN up to ≈20 pN. At the low end of the range (≈2–3 pN), the hairpins have higher probability to undergo thermally induced unfolding and thus are less suitable for cell force measurements. In contrast, hairpins are rarely found to have $F_{1/2}$ value greater than 20 pN because the free energy of hybridization provides diminishing returns for longer stem regions. This defines the range of forces that are detectable by conventional hairpin probes.

2.2. Mechanical Melting of DNA Duplexes

In contrast to DNA hairpins, separating a DNA duplex under force is irreversible because of the lack of connection that holds the two strands together. Stretching the same duplex with different orientations has a drastically different outcome despite having the same thermal melting temperature (T_m) and ΔG of duplex formation. Force-dependent dissociation of duplexes can be induced by stretching it along its axis (5′-5′, shearing geom-

etry, Figure 3C) or perpendicular to its axis (5′-3′, unzipping geometry, Figure 3C). Early SMFS experiments revealed that forces required to shear a DNA duplex linearly correlated to its length and approaches an asymptotic limit at a critical length of ≈30 bp.[37] In contrast, forces required to separate duplexes in the unzipping geometry tend to be much smaller because the external force applied is concentrated to break the nearest base pairs one by one in a stepwise fashion.[34,38]

There is rich experimental and theoretical work aimed at examining the mechanical stability of DNA duplexes in the unzipping and shearing geometry.[37,39] An interesting model proposed by de Gennes[39c] treats the DNA duplex as a ladder with springs connecting the nucleotides within the same strands and hydrogen bonding holds the interstrands together. For a duplex that experiences shearing forces at both ends (5′-5′), it is hypothesized that the applied force is only distributed to a finite number of base pairs at both ends, rather than distributing evenly across the whole duplex. Based on these assumptions, the tension tolerance (T_{tol}), required to melt 50% of the DNA duplex can be mathematically expressed as shown in Equation (4)

$$T_{tol} = 2 f_c \left[x^{-1} \tan h \left(x \frac{N}{2} \right) + 1 \right] \tag{4}$$

where f_c is the rupture force to break a single base pair (3.9 pN), $x = \sqrt{2R/Q}$ is a function describing the elasticity within the duplex—Q is a spring constant between neighbors within

ADVANCED
SCIENCE NEWS
www.advancedsciencenews.com

NANO · MICRO
small
www.small-journal.com

a strand, and R is a spring constant between base pairs in a duplex, N is number of base pairs formed within a duplex.

Alternatively, a duplex that experiences unzipping forces at the same end (5′-3′) breaks readily by relatively small forces. From this model, the unzipping force required to melt a duplex is estimated to be $\approx$12 pN.[40] For illustration, Figure 3D plots the rupture behavior of a 24 mer DNA duplex moving from an "unzipping" geometry to "shearing" geometry. x was experimentally determined by single molecule pulling experiments with a "clamp" time of 2 s at room temperature.[37] However, one caveat for this simplified model is that it does not account for the DNA duplex sequence, its GC content and more importantly, the time-dependent rate of mechanical denaturation, as this rate highly depends on the duration of the applied force. Interestingly, recent coarse-grained modeling[39e] and Monte Carlo simulation[41] suggest that typical DNA duplexes used for in vitro experiment ($N > 20$ bp) show weak dependence of rupture force on the duration of the applied force within biologically relevant time scales ($t = \approx$ s to min, Figure 3E). This is predicted to hold for both the "unzipping" and "shearing" geometry. Hence, the theoretical work by de Gennes still carries relevance for cellular force measurements.

3. DNA-Based Force Probes to Map Piconewton Forces Within Cells

DNA-based force probes are extracellular force sensors capable of reporting pN forces transmitted by cell surface receptors. These probes are immobilized to a substrate through one terminus, while the other terminus displays a biological ligand for cell receptor recognition. Cells transmit forces through their membrane receptors to the ligands on the DNA probes which causes DNA melting or conformational switching leading to enhancement, abolishment, or amplification in fluorescence signal, depending on the output mechanism (**Figure 4**). Broadly, MTFM probes can be classified as either reversible or irreversible probes. The reversible MTFM probes can in turn be divided into two main types: analog and digital. Analog probes display increasing levels of signal that is proportional to the magnitude of applied F. The best example of this category is the original PEG-based MTFM probe.[8] Biomolecules with secondary structure, such as proteins and DNA hairpins, are digital because of the cooperative nature of unfolding. The signal generated by irreversible tension probes is digital by design (Figure 4). Sections 3.1 and 3.2 provide further details pertaining to digital DNA probes.

One can view the DNA-based force probes under the umbrella of biosensors, where the analyte is the cellular force and its location; the transducer is the conformational change of a DNA nanostructure; and the output is the change in fluorescence signal associated with force-induced DNA conformational changes. Additionally, the DNA-based force probe fulfills many of the ideal characteristics of a biosensor. It displays high selectivity against forces transmitted by a particular cell surface receptor because the binding is mediated by specific receptor–ligand interactions; the surface chemistry for immobilization is well established and thus is highly reproducible; it has high sensitivity in terms of force resolution ($\approx$pN) as the unfolding

response is governed by the mechanical properties of DNA nanostructures; and it is relatively stable under cell imaging conditions. In this section, we will cover some of the achievements enabled by DNA-based force probes to study exciting questions in the realm of mechanobiology.

3.1. Force Probes Based on Dynamic DNA Hairpin Structures (Reversible Digital Probes)

Compared to the initial PEG-based molecular force probes that used an elastic (entropic) polymer as a force responsive module, dynamic nucleic acid nanostructures such as DNA hairpins are fundamentally advantageous for several reasons. First, unfolding of a simple DNA hairpin structure under forces is highly cooperative and this resembles a "digital" response. In contrast, stretching PEGs and elastic polypeptides under forces typically shows a graded "analog" response, where the extension, and hence the fluorescence due to dequenching, increases as a function of the magnitude of the externally applied forces (Figure 4A). Although entropic polymer-based probes are powerful to report force magnitude in continuum, estimating single receptor forces with these analog sensors is challenging. This is because the ensemble fluorescence signal generated by analog probes is difficult to interpret. For instance, the measured signal may be produced by very few receptors bearing large forces, or many of receptors that generate comparatively low force and these scenarios are degenerate. This issue can be resolved using single molecule fluorescence techniques as demonstrated recently by Dunn and co-workers.[42] That being said, single molecule imaging conditions require oxygen scavengers and high concentrations of reducing agents which are relatively toxic to cells. DNA probes based on the hairpin structure circumvent this problem because the force-induced unfolding response is "digital" responding to a threshold discrete force value (i.e., only forces larger than the $F_{1/2}$ of the hairpin probes can be detected), although this sacrifices their ability to distinguish cellular forces with magnitudes that are higher than the $F_{1/2}$. Accordingly, the fluorescence intensity is directly proportional to the number of unfolded probes, and the measured fluorescence signal quantifies the fraction of probes that are open. The absolute number of probe opening events can be quantified using a calibration standard, such as a supported lipid bilayer (SLB) with known fluorophore density.[43] Second, DNA hairpin structures have a well-defined force response which is tunable by modulating the ΔG of hybridization and stretching (i.e., changing the stem length and GC content, **Table 1**), in contrast to the force response of entropic probes which is purely dictated by the size of the "spring," and thus their contour length. Third, DNA synthesis is highly modular allowing a variety of functional groups to be introduced during on-column synthesis or post modification at costs that are continuously dropping. Lastly, the use of well-defined DNA structures places the fluorophore in close proximity to the quencher [quenching efficiency (QE) = $\approx$90–95%], and this in turn generates high signal-to-background ratio when the probe is open. For reference, typical QE for a fluorophore–quencher pair in entropic-spring based force probes is $\approx$70% at best due to their random coil structure. Overall, these advantages make

ADVANCED
SCIENCE NEWS
www.advancedsciencenews.com
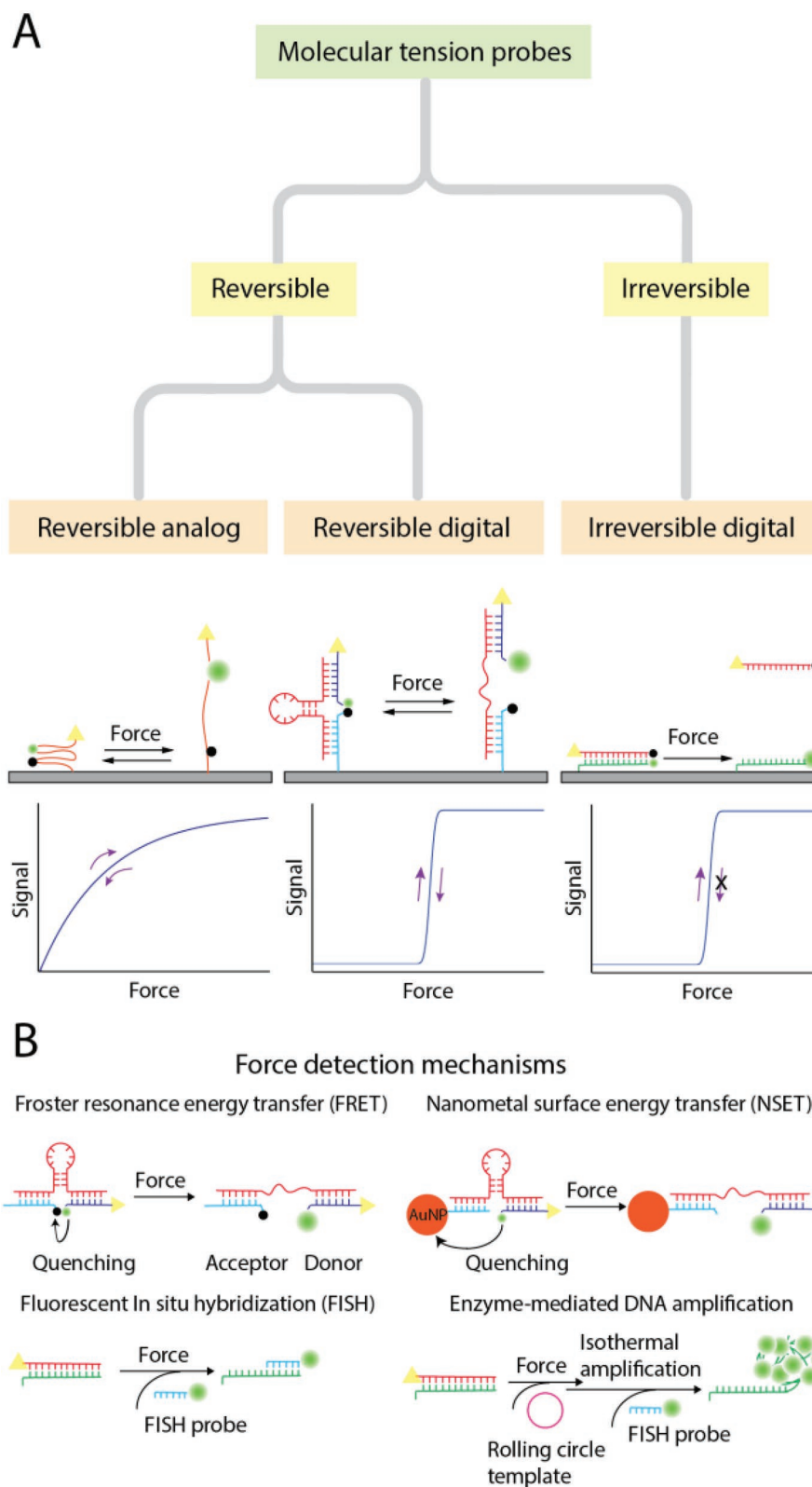
NANO · MICRO
small
www.small-journal.com

Figure 4. A) Classification of different types of molecular tension probes based on their reversibility and the expected change in fluorescence signal as a function of applied force. The reversible analog force sensor uses an elastic entropic material (e.g., polyethylene glycol or elastic polypeptide) as a spring. The reversible digital force sensor consists of a re-foldable secondary structure (e.g., DNA hairpin stem-loop). The irreversible digital force sensor is composed of a DNA structure (e.g., DNA duplex) that cannot refold upon rupturing. B) Representative examples of fluorescence detection mechanisms that can be used to detect force-induced structural change of the DNA-based force probe.

Table 1. Representative thermodynamic and mechanical parameters of hairpin structures used for the construction of DNA hairpin-based force probes.

GC content [%]	Stem size [bp]	Loop size [nt]	ΔG_{fold} at 25 °C [kJ mol^{-1}][a]	Calc. $F_{1/2}$ at 25 °C [pN][b]	ΔG_{fold} at 37 °C [kJ mol^{-1}][a]	Calc. $F_{1/2}$ at 37 °C [pN][b]	Exp. $F_{1/2}$ [pN]
22	9	7	23.3	7.8	12.8	5.9	4.7[c]
30	10	4	33.3	10.1	22.5	8.0	8.1[d]
35	20	4	90.8	12.0	68.9	10.0	11.3[d]
77	9	7	52.3	13.6	40.6	11.3	N.D.
100	12	4	100.9	20.2	86.1	17.8	13.1[c]
100	20	4	170.5	19.8	143.9	17.4	19.3[d]

[a]Estimated using IDT oligo-analyzer tool and only the ΔG of the most stable conformer is listed. Conditions used for the predictions: 137.3 ×10^{-3} M NaCl, 0.8 ×10^{-3} M MgCl₂ [b]Estimated using Equation (3). Persistence length of ssDNA is assumed to be 1.3 nm and contour length of ssDNA is 0.63 nm per nucleotide [c]Biomembrane force probe calibration at 25 °C and 137.3 ×10^{-3} M NaCl [d]Optical tweezer calibration at 25 °C, and 200 ×10^{-3} M KCl. N.D. = not determined.

DNA-based hairpin probes as promising alternatives for mapping forces in the living systems.

3.1.1. Force Probes Assembled from Multiple DNA Strands

The first generation of DNA force sensors for cells were comprised of a surface anchoring strand labeled with a quencher, a ligand strand modified with a fluorophore and a hairpin strand complementary to the other two. In the resting state, the fluorophore and the quencher are placed in close proximity. When cell receptors recognize their cognate ligands and pull with a force larger than the $F_{1/2}$, the stem-loop structure unfolds, thus separating the fluorophore from the quencher and resulting in restoration of fluorescence emission (**Figure 5**A). The generated fluorescence signal indicates the location where receptors actively transmit pN forces above the $F_{1/2}$ of the hairpin. This

"three-component" system is facile to prepare because each element is synthesized separately; the force response, anchoring, and ligand elements are unique oligonucleotides. Using this approach, one can quickly create a library of hairpin probes with different $F_{1/2}$ values without the need for cumbersome multistep resynthesis and purification.

The integrin family receptors are the most common cell adhesion receptors and found in many cell types. Adherent cells such as endothelial, epithelial, and fibroblasts recognize the extracellular matrix (ECM) using integrins, and then form a specialized cellular architecture called a focal adhesion (FA). Integrins within FA complexes are responsible for transmitting traction forces to specific ECM ligands and are essential for the subsequent mechanical signaling (mechanotransduction). To map integrin force transmission and subsequent signaling, we used three-component hairpin probes in live cells.[10] In proof-of-concept experiments, we seeded
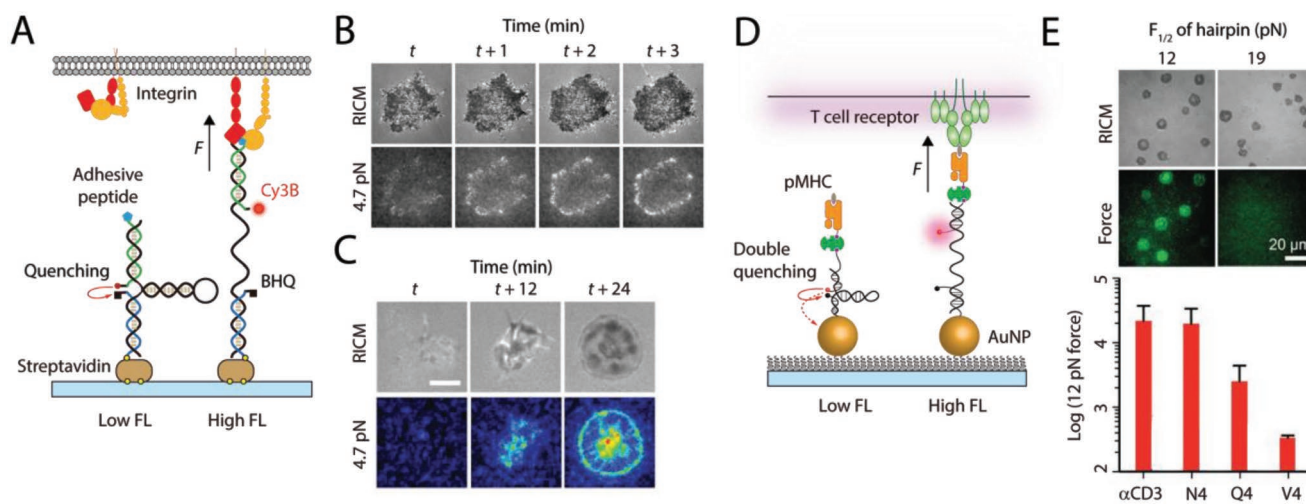

Figure 5. DNA hairpin-based force probes. A) The DNA force probe consists of three oligonucleotides to form the sensor and is immobilized on a glass surface via biotin–streptavidin interaction. This probe is decorated with a fluorophore and quencher and a biological ligand to report the force-induced hairpin unfolding by a cell. B) Time-lapse images showing the spatiotemporal change in spreading and the force signal of a NIH-3T3 fibroblast cell. Reproduced with permission.[10] Copyright 2014, Springer Nature. C) Time lapse images of a spreading human platelet and associated integrin tension signal. Reproduced with permission.[44] Copyright 2018, National Academy of Sciences, USA. D) Studying T cell receptor forces with a DNA-based AuNP force probe with increased sensitivity and stability. E) Spreading of naïve OT1 cells on tension sensing substrate where the DNA force probes are decorated with N4 pMHC. These cells were unable to open probes with $F_{1/2}$ = 19 pN (Top). Bar chart showing force responses of Naïve OT1 cells encountering different antigens (Bottom). Reproduced with permission.[46] Copyright 2016, National Academy of Sciences, USA.

**ADVANCED
SCIENCE NEWS**
www.advancedsciencenews.com

NANO · MICRO
small
www.small-journal.com

cells on a substrate presenting three-component force probes. Cells recognized the Arg-Gly-Asp (RGD) peptide on the force probes and generated fluorescence signals coincident with the markers of the FA complexes (Figure 5B). We validated the force signals using cytoskeletal inhibitors which caused cessation of fluorescence signals, suggesting probe refolding. These results showed unfolding of hairpin probes was tightly regulated by the forces transmitted via the cytoskeleton of cells. Importantly, these DNA-based force probes enabled multiplex force measurement within integrin clusters that cannot be resolved using TFM. Using spectrally encoded tension probes with different $F_{1/2}$ values (4.7 and 13.1 pN), we showed that forces within a single FA distributed unevenly, and a subset of integrins pulled with a force that is lower than 13.1 pN but greater than 4.7 pN.

This hairpin force probe technology was recently adapted to investigate the spatiotemporal distribution of integrin forces during platelet activation,[44] which is a key initial event in blood clotting. We found that platelets used their $\alpha_{IIb}\beta_3$-integrins to generate two populations of force patterns: a central zone with integrin forces >19 pN and a ring of peripheral forces along the lamellipodial edge with the magnitudes between 4.7 and 13.1 pN (Figure 5C). Drug inhibition experiment revealed these forces indeed were regulated by two separate biochemical signaling pathways associated with myosin light chain kinase, which has a role in maintaining the forces at the cell edge, and Rho-associated protein kinase, which regulates the stabilization of central contractile forces. Note that imaging platelet traction forces is very challenging because of their small size ($\approx$few μm^2). Previous attempts to image platelet forces using TFM failed to reveal the ring and central zone pattern of traction forces.[45] More importantly, we also discovered that exposure of phosphatidylserine (PS), which results in generation of thrombin and its subsequent coagulation cascade for blood clotting, proceeds after cessation of the integrin mechanical signaling in platelets, indicating that mechano-biochemical signaling contributes to the clot forming process.

To increase the sensitivity of DNA-based MTFM probes, we employed gold nanoparticles (AuNPs) for probe immobilization (Figure 5D).[46] In this approach, the DNA-based hairpin probe was functionalized with a terminal thiol group enabling the formation of a gold–thiol bond, which can resist rupture forces up to few nN.[47] The key advantage of this approach is the dual quenching due to the energy transfer from the fluorophore to the metal surface, as well as the molecular quencher.[48] Combining two quenching mechanisms in this design, we found that unfolding of hairpin probes can generate up to a 100-fold fluorescence enhancement and thus are more sensitive than the original design which displayed a $\approx$20-fold maximum fluorescence increase. This improved method was used to study the very first step of T cell activation. Antigen recognition by the T cell receptor (TCR) is vital to elicit potent adaptive immune response. DNA-based force probes revealed that T cells used their cytoskeleton to transmit forces to the TCR during antigen recognition, and these forces are highly transient and dynamic in nature. Unlike integrin molecules, the TCR actively transmits a surprisingly narrow range of forces (12–19 pN) to its cognate antigen (Figure 5E). When mutant peptide antigens

were displayed on the DNA probes, TCR forces were diminished, implying that mechanics are important in antigen discrimination (Figure 5E). Interestingly, a very recent study by Zhu and co-workers used DNA-based tension probes to show that thymocytes (progenitor of T cell) also harness mechanical energy for ligand sensing during early thymopoiesis, which dictates phenotypic outcomes in T cells.[49]

3.1.2. Force Probe Comprised of a Single Oligonucleotide

Coincident with our initial work of DNA-based MTFM probes, Chen and colleagues reported a similar method to generate hairpin-based force probes.[50] In their approach, the RGD peptide ligand, fluorophore and quencher, and a reactive group for surface anchoring were installed in a single stranded oligonucleotide that forms a hairpin stem-loop. This probe was covalently grafted to a surface via thiol-maleimide coupling. Fibroblast cells were used as a model system for their study and showed similar conclusions to our work, where the fluorescence signals were exclusively observed at the FA complexes and the force distribution by integrins was highly heterogeneous within a single FA. In comparison to our three-component DNA hairpin probe, this design is more robust, and hence it is amenable to imaging tension for longer time scales. Note that we have previously developed PEG-based MTFM probes that displayed increased stability, but DNA probes are particularly sensitive to nucleases present in cell culture conditions. Despite the increased potential stability, the single component DNA-based force probe has not been used in the intervening years due to the complexity of synthesis.

3.2. DNA Probes to Control Peak Receptor Tension (Irreversible Digital Probes)

The tension gauge tether (TGT) was originally developed by Wang and Ha, in 2013, to control the magnitude of peak tension experienced by receptors.[40] TGT is a ligand labeled DNA duplex tailored to dissociate at force levels exceeding its T_{tol}. As defined in Figure 3C,D, T_{tol} of the TGTs can be fine-tuned by varying the ligand anchoring position. Receptor forces larger than the T_{tol} rupture the tether, and hence abolish mechanical signaling. In contrast, mechanical forces lower than the T_{tol} are maintained (**Figure 6**A). With the aim of defining the force magnitude required to activate a biophysically induced signaling cascade, Wang and Ha designed nine RGD-TGTs with T_{tol} ranging from 12 to 58 pN, and showed that these mechanically different, chemically similar DNA probes (with same T_m and ΔG of hybridization) had profound effects on integrin mediated mechanotransduction. They tested this system with several cell lines and concluded that a universal threshold force of $\approx$40 pN was required for integrin mediated activation and initial cell adhesion. Interestingly, although the 43 pN TGTs supported initial cell adhesion, these cells failed to form robust FAs and stress fibers. On the other hand, cells seeded on the 56 pN TGTs allowed the formation of mature FAs and stress fibers. Therefore, they concluded that larger forces are
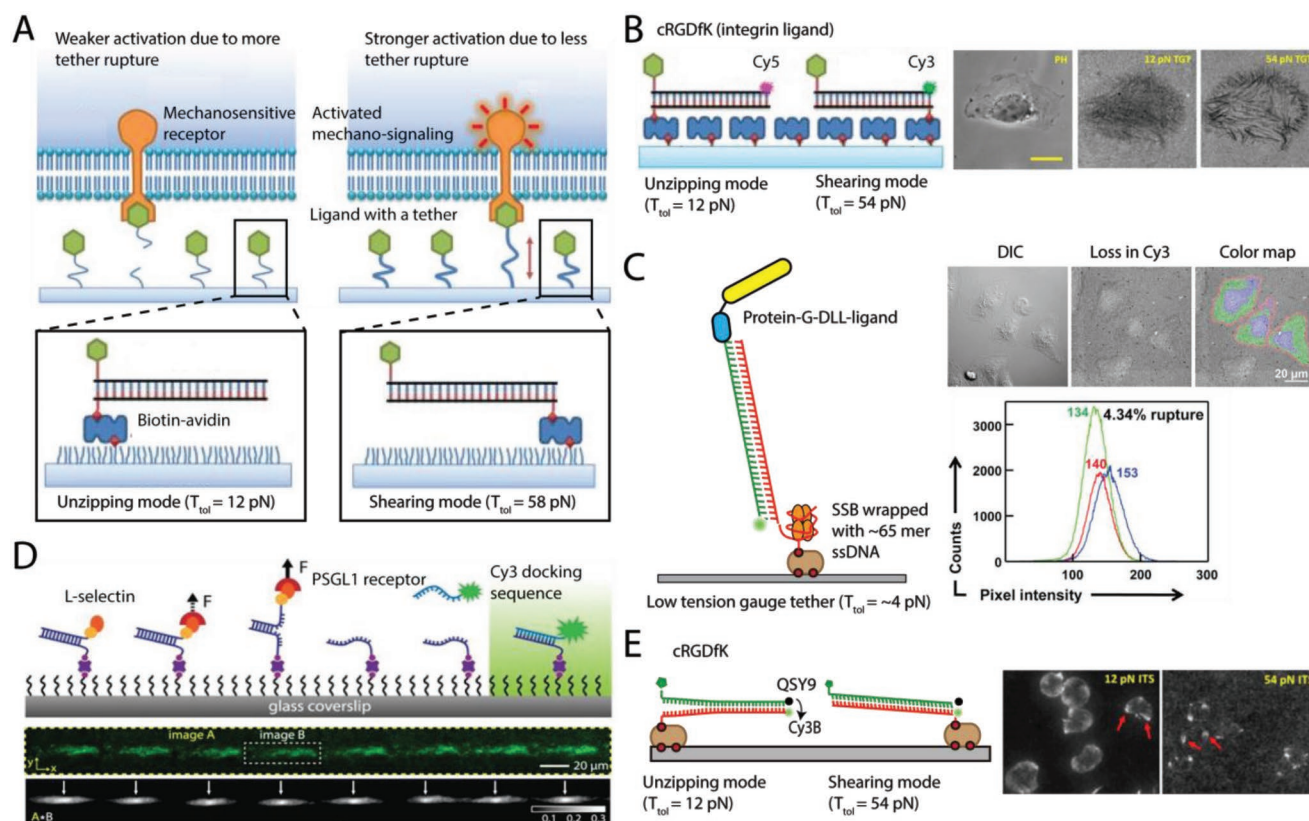
Figure 6. DNA-based tension gauge tether (TGT) and its variants. A) TGTs are rupturable DNA duplexes presenting ligands on a surface. A specific rupture force of the duplex (T_{tol}) can be estimated depending on the force application geometry (see Figure 3C–E and Equation (3)). Mechanical denaturation of TGTs occurs when the receptor forces exceed the T_{tol}. The force required for cell attachment or activation can be determined using a range of TGTs with increasing T_{tol}. Reproduced with permission.[40] Copyright 2013, American Association for the Advancement of Science. B) "Turn-off" TGTs are made of fluorescently tagged ligand strand. Mechanical denaturation of TGTs generates loss of fluorescence signal on the surface which can be used to map the spatial distributions of integrin forces (Left). Phase contrast (PH) and fluorescence imaging of a CHO-K1 cell spreading on the multiplexed TGT surfaces. Cells spread on 54 pN TGT surface generated organized patterns that mimic the focal adhesion complex, while cells spread on the 12 pN TGT surface had a disorganized pattern. Scale bar = 10 µm (Right). Reproduced under the terms and conditions of the Creative Commons Attribution License 4.0.[53] Copyright 2016, The Authors, published by Springer Nature. C) Low TGT (LTGT) reports forces at a lower regime. A ssDNA overhang is wrapped around a homotetrameric single-tailed SSB and can be unspooled at a force of ≈4 pN. The DNA duplex is decorated with a biological ligand for cell recognition and a dye to report loss of fluorescence upon cell pulling (Left). Loss of LTGT fluorescence after incubating the CHO-K1 cells expressing Notch receptors on the surface for 2 h. Red, green, and blue regions indicate background, rupture region, and cell nuclei, respectively (Right). Reproduced with permission.[54] Copyright 2016, American Chemical Society. D) Fluorescence in situ hybridization (FISH) based TGTs utilize the exposed ssDNA strand, resulting from TGT rupture, as a docking sequence. Complementary Cy3B strand flowed into the chamber hybridizes with the docking sequence and generates a "turn-on" signal visualizable with total internal reflection fluorescence microscopy (Top). Adhesion footprint of a rolling leukocyte reveals periodicity of the rolling adhesion mediated by the PSGL1 receptors (Bottom). Reproduced under the terms and conditions of the Creative Commons Attribution License 4.0.[56] Copyright 2017, The Authors, published by Springer Nature. E) Quantitative TGT (or integrative tension sensor, ITS) consists of a pair of a fluorophore and quencher that are labeled on the TGT. Rupture of the TGT generates a permanently "turn-on" signal on the surface that can be used to track the spatial distributions of receptor forces (Top). Fluorescent imaging of mouse platelet cells reveals that these cells specifically pull with integrin forces >54 pN at the cell periphery (Bottom). Reproduced with permission.[58] Copyright 2018, Elsevier.

needed for sustaining biophysical signaling of integrins. They also used this intriguing platform to test the force required for activation of Notch signaling and found that both the 12 and 58 pN TGTs support efficient Notch activation, suggesting Notch activation may be insensitive to mechanical forces or the activating force is below 12 pN. Since then, significant progress has been made toward developing more generalizable TGT probes for the community, including the development of protein G-TGTs to present Fc-fused functional protein ligands with a specific conformation,[51] and the development of an

easy-to-implement protocol for tethering TGT probes on regular cell culture dishes.[52]

3.2.1. "Turn-Off" TGT Probes to Map Peak Tension

In 2016, Wang and co-workers synthesized "turn-off" TGT probes to provide a readout of the peak forces using fluorescence microscopy. These "turn-off" TGTs showed the magnitude and spatial distribution of maximum integrin forces

exceeding T_{tol} (Figure 6B).[53] This system employed a DNA oligonucleotide presenting the RGD peptide ligand at one terminus and a fluorescent dye conjugated to other terminus. When cells were seeded on the "turn-off" TGT surface, receptor forces larger than T_{tol} ruptured TGTs resulting in the loss of fluorescence. Five "turn-off" TGTs with T_{tol} ranging from 12 to 54 pN were used here and reconfirmed that forces >40 pN were required for efficient cell spreading but not for initial cell adhesion. Interestingly, they showed that cells were able to rupture the strongest 56 pN TGT with spatially organized force patterns despite being adhered to the substrate.

Rupturable DNA-based force probes can also be designed relying on the affinity between a DNA binding protein and DNA. One such example is the Escherichia coli. ssDNA binding protein (SSB), which can bind a long poly-T DNA forming a thermodynamically stable product. Ha and coworkers exploited this phenomenon and hypothesized this binding could be disrupted by pN forces.[54] They determined from optical trap experiments that application of only ≈4 pN force was sufficient to peel a 65 nt poly-T ssDNA off from this ssDNA binding protein. Following this observation, they constructed a new generation of TGTs with lower T_{tol} (LTGT) to define the forces required for Notch Activation. One end of the TGT presents a long ssDNA overhang for binding the ssDNA binding protein. The other end consists of a short DNA duplex tethering with DLL4-ligand for receptor recognition (Figure 6C). Surprisingly, no apparent activation of Notch signaling was observed when cells were plated on these LTGT probes even for 48 h, while 12 and 56 pN TGT probes enabled robust Notch activation. This suggests Notch receptor physically tugs on its cognate ligand with 4–12 pN force and this is associated with endocytosis of the ligand by the signaling cell. In another report, Garcia and co-workers utilized the LTGT probe to show that mechanical tuning of Notch receptor signaling can be altered by manipulating the binding affinity of the receptor–ligand interaction.[55] They identified that a mutated Notch ligand Jag1-JV1 has greatly enhanced binding affinity to Notch receptor. Interestingly, wild-type Jag 1 tethered to LTGT probes could not activate Notch signaling, while activation of Notch was robust when Jag1-JV1 or DLL-4 LTGT probes were used. The different mechanical response implies that the Notch receptor uses forces to discriminate ligands, and the receptor forces were harnessed to tune the overall strength of the biochemical signaling.

3.2.2. Turn-On TGT to Map Peak Receptor Tension

In 2017, an interesting strategy was reported by Chemla and co-workers where they directly used the surface immobilized single stranded DNA, resulting from TGT rupture, as a docking sequence for fluorescent in situ hybridization (FISH) (Figure 6D).[56] Here, a P-selectin ligand was chemically modified onto the TGT with T_{tol} of 12 pN to visualize the rolling adhesion of leukocytes, mediated by the PSGL receptor, under shear flow conditions. From this assay, the authors discovered a periodically patchy, yet highly asymmetrical pattern of the adhesion footprint generated by TGT rupture and the subsequent FISH probe binding, while no such patterns were formed in

their control experiment where a rolling bead was used. This result suggested that the PSGL receptor on leukocytes may distribute unevenly across the whole cell surface. This feature is hard to resolve with TFM because the rolling behavior is rapid, and the rolling cell–surface contact is extremely small and approaches the spatial resolution of conventional TFM (≈1 μm).

Another approach to achieve "turn-on" fluorescence is the integrative tension sensor (ITS), or simply the "quantitative" TGT.[57] In this approach, the ligand presenting DNA strand is chemically coupled to a quencher while the surface anchoring strand is modified with a fluorophore and is placed in close proximity to the quencher, thereby quenching the emission of the fluorophore in the resting state. Integrin forces larger than the T_{tol} of TGT rupture the probe and remove the quencher from the surface, leading to generation of permanent "turn-on" signal (Figure 6E). In 2018, Wang and co-workers[58] reported this strategy to map the traction forces generated by platelet during initial adhesion and activation. Similar to the finding using DNA-based hairpin probes,[10] platelets used two force generating machineries in mediating TGT dissociation. One exclusively located at the cell edges with forces >54 pN and weaker force >12 pN that spanned across the cell surfaces. Importantly, Wang and co-workers showed that actomyosin contraction was responsible for generating >54 pN integrin forces but not the weaker forces. In a subsequent report, Wang and co-workers used ITS to study the magnitude and spatiotemporal dynamic of the integrin forces in migrating cells.[59] Using keratocytes as a model system, the authors revealed that these cells generated forces >54 but <100–150 pN during rapid migration. These forces were exclusively produced at the rear margins and sides of the cells and were postulated to have a role in promoting cell rear retraction to facilitate cell migration. Unlike platelet, immune cells and fibroblast, the source of these extremely high forces could be from actin treadmilling that stretches the cell membrane and generates a pulling force from de-adhesion rather than the actomyosin contraction.

3.3. Force Probe Equipped with Signal Amplification Mechanism

Inspired by the ELISA and PCR assays that revolutionized molecular biology, our lab developed a catalytic amplification strategy to convert mechanical forces into an amplified fluorescent readout, coined mechanically induced catalytic amplification reaction (MCR).[60] In initial proof-of-concept experiments, MCR leveraged the TGT as a peak force transducer. When integrins mechanically rupture the RGD-TGT, a ssDNA is exposed that serves as a primer for rolling circle amplification, a nucleic acid amplification technique to generate ssDNA with long-tandem repeats. The formation of this force-induced amplicon can be readily detected by methods such as FISH (**Figure 7**A). The product of MCR could either be detected using a fluorescence microscope or a plate reader, where the fluorescent probes are washed off from the surface and transferred to a 96 well plate for high throughput detection. We showcased the readout to measure the dose-dependent dissipation of actomyosin contractile forces by cytoskeletal drugs, and
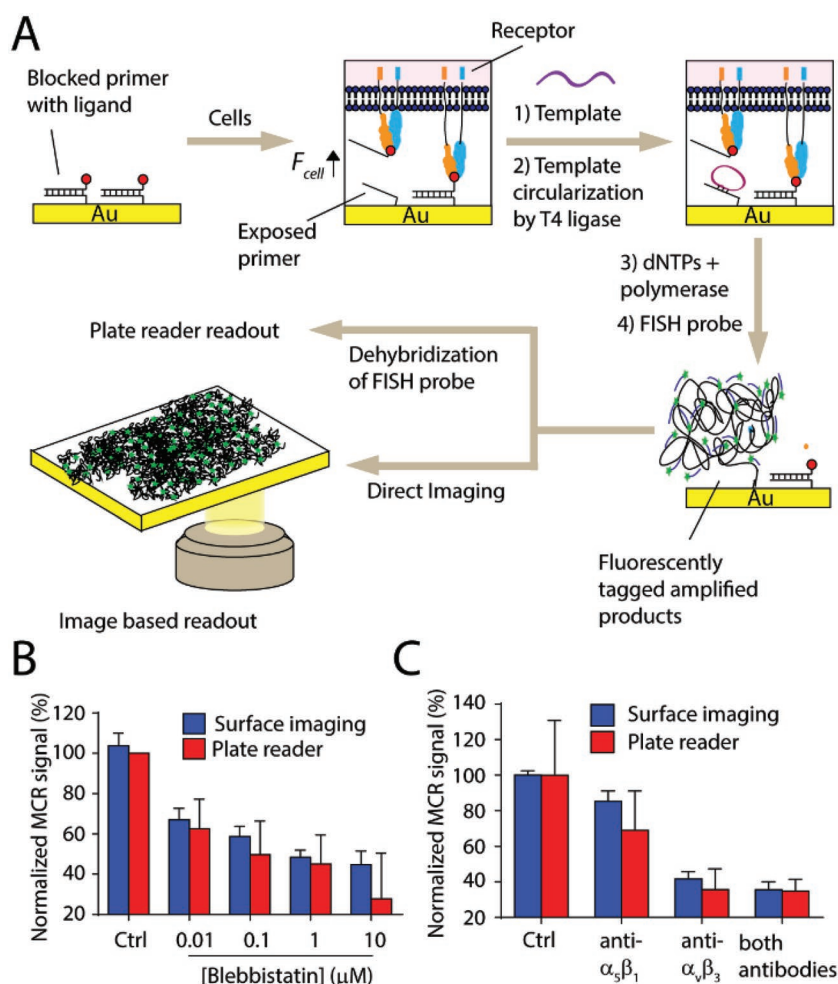
Figure 7. A) Mechanically induced catalytic amplification reaction (MCR) uses enzymes to convert the exposed primer, resulting from TGT rupture, into amplified fluorescence readout that can be detected either by fluorescence microscopy or a plate reader. B) Bar graph showing dose-dependent inhibition of myosin II activity by MCR. C) Bar graph showing the ability of MCR to differentiate integrin antibodies that block different integrin subtypes. Reproduced with permission.[60] Copyright 2016, Wiley-VCH.

that some receptors are thought to be anisotropic mechanosensors that differentially respond to forces based on their orientation, it is highly desirable to develop tools that can determine both the magnitude and direction of molecular forces applied by cells. To solve this problem, we and the Mattheyses lab coupled fluorescence polarization microscopy with the DNA hairpin force probes to enable direct measurement of integrin tension and force orientation.[61] Though a series of measurements, it was shown that the Cy3B fluorescence dye stacks on the terminal base pair of the DNA duplex, and thus the orientation of the dye is dictated by the orientation of the DNA duplex. Excitation-resolved fluorescence polarization can be used to deduce the orientation of the DNA hairpin and the applied forces (**Figure 8**A). This approach, called molecular force microscopy (MFM), also benefitted from mechanoselection, which is the suppression of Cy3B signal from probes that are at rest, thus reducing background. MFM showed that integrin molecules on platelets exhibited force orientations organized toward an axis rather than displaying isotropic contraction as shown by traditional TFM measurement.[45a] Further experiments identified that two spatially distinct regions of platelet traction forces exist during platelet activation (Figure 8B). Interestingly, when a group of aggregated platelets contracted, the integrin forces oriented separately toward a central axis in each cell, instead of pulling in a coordinated fashion toward a shared central axis of the clot.

3.5. Multivalent, Origami-Based Force Probe

DNA origami has emerged as one of the most promising "bottom-up" programmed self-assembly techniques for the creation of functional nanomaterials.[62] DNA origami nanostructures have been used to trigger multivalent receptor binding in living cells.[63] Given the intimate connection between receptor oligomerization, mechanotransduction and signaling, we and the Ke lab recently reported a new generation of origami-based force probes. These probes allow presentation of multiple ligands in a distance defined manner and also with more tunable $F_{1/2}$ values.[64] This probe utilized a six-helix bundle DNA origami as the "body." The top part of this origami body was functionalized with RGD ligands at an intermolecular spacing of ≈6 nm, while the bottom part of the body was linked to one, two or three DNA hairpin force probes (**Figure 9**). SMFS calibration showed that increasing the number of the same hairpin probes attached to the origami body enhanced the collective unfolding force. These probes were able to report platelet traction forces similar to the three component hairpin probes. Increasing the ligand density (presenting two peptides on the origami probe) while
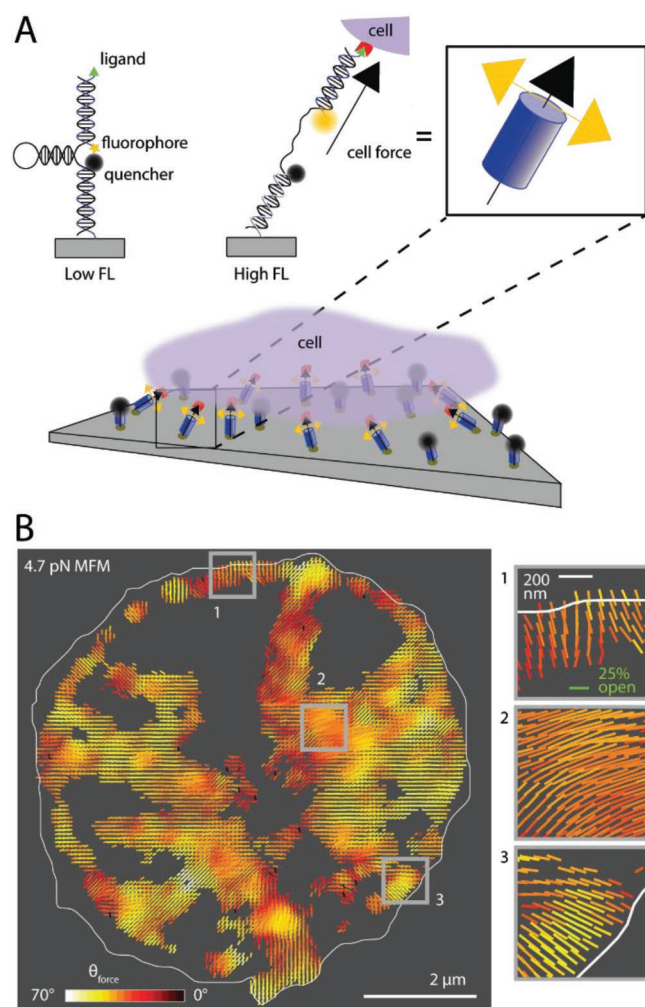
also its utility in differentiating antibodies that inhibit different integrin subtypes (Figure 7B,C). It is worth to note that unlike the aforementioned DNA hairpin probes which are capable of measuring receptor forces in real time, or TGTs that detect the history of force generation, the MCR signal is highly dependent on the duration of cell incubation that alters the number of ruptured probes, as well as the amplification conditions (e.g., enzyme concentration, primer concentration, etc.). Therefore, MCR signal does not provide an absolute readout of mechanical events and requires proper calibration and controls, much like conventional ELISA and PCR assays.

3.4. Force Probe Enabling Measurement of the Force Orientation

One challenge for the DNA-based MTFM technology is that it only provides readout of the magnitude of receptor forces. Given

Figure 8. Molecular force microscopy (MFM) maps the direction of receptor-mediated forces. A) MFM relies on the use of fluorescence polarization in conjunction with the DNA hairpin-based force probes. As the Cy3B dye is stacked parallelly with the terminal base on one end of the duplex, its orientation can be resolved by polarized excitation light. B) Representative MFM map of platelet integrin forces. Color of the lines indicates θ_{force} relative to the z coordinate. Reproduced with permission.[61] Copyright 2018, Springer Nature.

maintaining the probe density significantly enhanced the force signal and spreading area of the platelets, presumably due to the increased probability of integrin binding to its ligands.

3.6. Force Probes on Fluid Membrane Interfaces

In multicellular organisms, cells utilize an array of molecular mechanisms to communicate with one another for survival. One such important molecular mechanism for signal transduction is juxtacrine signaling (also known as contact-dependent signaling), which requires two interacting cells to form a direct physical bridge using a membrane anchored receptor and its surface ligand. This is in contrast to the more conventional endocrine and paracrine signaling pathways in which the activation of a receiving cell relies on binding of a soluble molecule

secreted by the signal-sending cell. The information exchange process within intercellular junctions is further complicated by the interplay between many receptor–ligand pairs that tend to laterally oligomerize, signal and in many cases experience mechanical forces.[65]

SLB formed on a solid substrate[66] provides a robust experimental platform for studying signaling at the cell–cell junctions[67] and bioanalytical[68] applications. SLBs retain certain key characteristics of live cell membranes including high lateral fluidity, chemical compositions that resemble those of plasma membrane and compatibility toward an array of membrane components. SLBs allow membrane inserted components or tethered ligands to move and assemble into functional assemblies while retaining their biological activities. Therefore, SLBs can act as a model cell membrane to study juxtacrine signaling.

DNA-based force probes that are physically affixed to a solid support do not fully reconstitute the physical characteristics of intercellular junctions formed between two cells, where the receptor–ligand complexes rearrange in space and time to form functional, multicomponent assemblies to modulate the signaling strength.[69] One archetypical example is the interface formed between a T cell and the antigen presenting cell, which is called the immunological synapse (IS). At this intercellular junction, the TCR binds to its antigenic pMHC on the target cell which leads to formation of small TCR-pMHC clusters. Over a duration of a few minutes, multiple signaling and adhesion molecules are spatially organized into distinct micron scale zones that facilitate the signaling function of T cells.[70]

To better mimic this biophysical observation and study the dynamics of TCR forces during the formation of the immunological synapse, we tethered DNA hairpin tension probes on SLBs that allow concurrent measurement of TCR forces and lateral clustering of TCR-pMHC complexes (**Figure 10**A).[71] These force probes include two fluorescence reporters, one that reports on clustering and was insensitive to DNA hairpin unfolding, and the second fluorophore that reports on mechanical forces and probe clustering. By taking the ratio of these two signals, one can normalize for the mechanical force per TCR–pMHC complex. Using these ratiometric force probes labeled with anti-CD3ε antibodies, we showed that TCR experienced forces >4.7 pN during lateral translocation in a myosin IIA dependent fashion, and a subset of TCRs exerted force at the center of mature immunological synapse structure, which may be associated with endocytosis of antigen (Figure 10A).

Membrane-anchored DNA force probes were also recently applied to study B cell mechanobiology. Immune cells such as B cells help destroy microbes by producing antibodies that bind their antigens. To elicit clonal expansion and potent antibody responses, B cells use their B cell receptor (BCR) to recognize foreign antigens on antigen presenting cells. During B cell activation, BCR binds to the antigen and triggers the formation of IS, leading to antigen extraction and reprocessing for the helper T cells. Previous work showed that B cells use mechanical energy to discriminate antigen quality.[72] However, the magnitude of these extraction forces was unknown. To address this question, Tolar and co-workers employed ratiometric DNA hairpin tension probes to investigate force generation of B cells at the cell–SLB junction (Figure 10B). This study aimed at comparing the mechanical state of B cells with
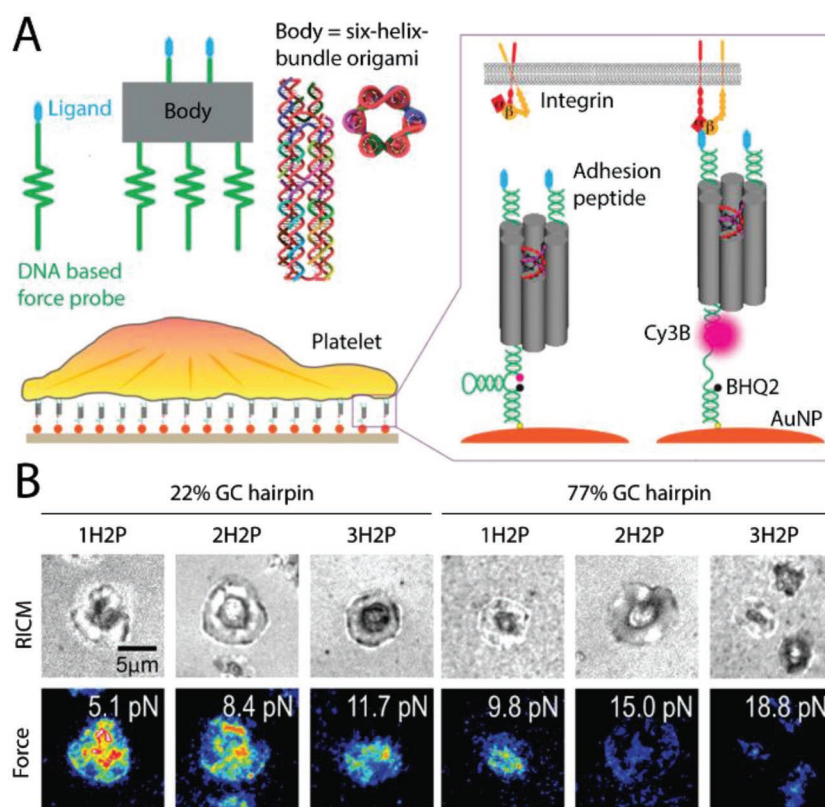
ADVANCED
SCIENCE NEWS
www.advancedsciencenews.com

NANO · MICRO
small
www.small-journal.com

Figure 9. A) Schematic showing the design of DNA origami-based force probes. A six-helix bundle origami is used as a body to link multiple DNA hairpin force probes and biological ligands. The unfolding of these probes is dictated by a collective $F_{unfolding}$ calibrated by SMFS. B) RICM and fluorescence imaging reveal human platelets pull on origami force probes with increasing $F_{unfolding}$. Reproduced with permission.[64] Copyright 2018, American Chemical Society.

different origins—germinal center B cells and naïve B cells.[73] To achieve this goal, the ratiometric hairpin probes were decorated with anti-Igκ antibodies allowing probe recognition by the B cell receptors. Using hairpins with different unfolding forces, the authors revealed that germinal center B cells generated stronger forces compared to naïve B cells (Figure 10B). This observation could presumably be explained by the smaller receptor–ligand clusters and higher myosin II activity found in germinal center B cells, where they exploited this force-dependent mechanism to achieve affinity discrimination of BCR ligands. Very recently, Pierce and co-workers used this ratiometric force probe to compare force generation of naïve B cells and light zone germinal center (LCGC) B cells. They discovered that naïve B cells accumulated the probe at the center of cell–SLB contact and BCR transmitted forces <9 pN, while LCGC B cells arrested the probes into small clusters, and the BCRs within the clusters generate forces >9 pN.[74]

An interesting development in the area of membrane-tethered DNA probes is a class of probes that physically bridges two cells. To map mechanical forces transmitted at the junction between two living cells, You and co-workers modified the anchoring terminus of the DNA hairpin tension probe with a pair of cholesterol moieties, so that the probes can be spontaneously assembled on a cell surface with high kinetic stability

(Figure 10C).[75] This design was used to investigate intracellular tension of E-cadherin and integrin receptors. The authors showed that the fluorescence at the cell–cell junction was significantly higher than the other parts of a cell without contact, presumably caused by hairpin unfolding by the neighboring cell. Future studies that incorporate a ratiometric or FRET reporter to control for probe density is needed. Alternatively, fluorescence lifetime imaging microscopy (FLIM)[76] will also help differentiate the contribution of probe clustering from hairpin opening.

4. Conclusion and Perspective

Within the past six years, DNA-based force probes have emerged as a versatile biophysical toolkit for studying cellular mechanotransduction. This technique uniquely weds the strengths of SFMS (≈pN force resolution) and TFM (whole cell force measurement) and has garnered significant interest from the community. We have reviewed the mechanical properties of two main classes of DNA tension sensors—DNA hairpins and DNA duplexes and how they can be employed as force probes to "passively observe" or "actively manipulate" cellular mechanotransduction. We have also highlighted innovative method development such as "mechano-PCR" (MCR), "mechano-FISH," molecular force microscopy and origami-based force probes to improve the capabilities in mechanobiology (i.e., improved signal-to-noise during observation, full characterization of the direction of the receptor force, and more controllable and tunable unfolding force of the spring). While this field is still in its infancy, we will need to refine and expand the toolbox to allow easier adaptation for more diverse scientific communities.

Apart from the DNA hairpins and duplexes, noncanonical DNA structures with better mechanical stabilities should enable spatiotemporal detection of surface receptors that generate high forces in real time. Noncanonical DNA structures such as G-quadruplex[77] and i-motif[78] were demonstrated to have relatively higher unfolding forces (≈20–40 pN measured by OT) compared to DNA hairpins. Similarly, OT measurement of DNA origami nanotubes revealed that these structures could be mechanically unfolded with forces of ≈40–50 pN.[79] Because these structures also unfold cooperatively like the DNA hairpins, they can potentially be harnessed as "stiffer springs" for reversible force probe design. However, the rupture forces of naturally occurring nucleic acids are fundamentally limited because of their relatively weak hydrogen bonding interactions. To further increase the mechanical stability, and thus to push for a wider applicability in biological systems and material science, xeno nucleic acid (XNA) with improved mechanical stabilities may fulfill this challenging task. For example, peptide
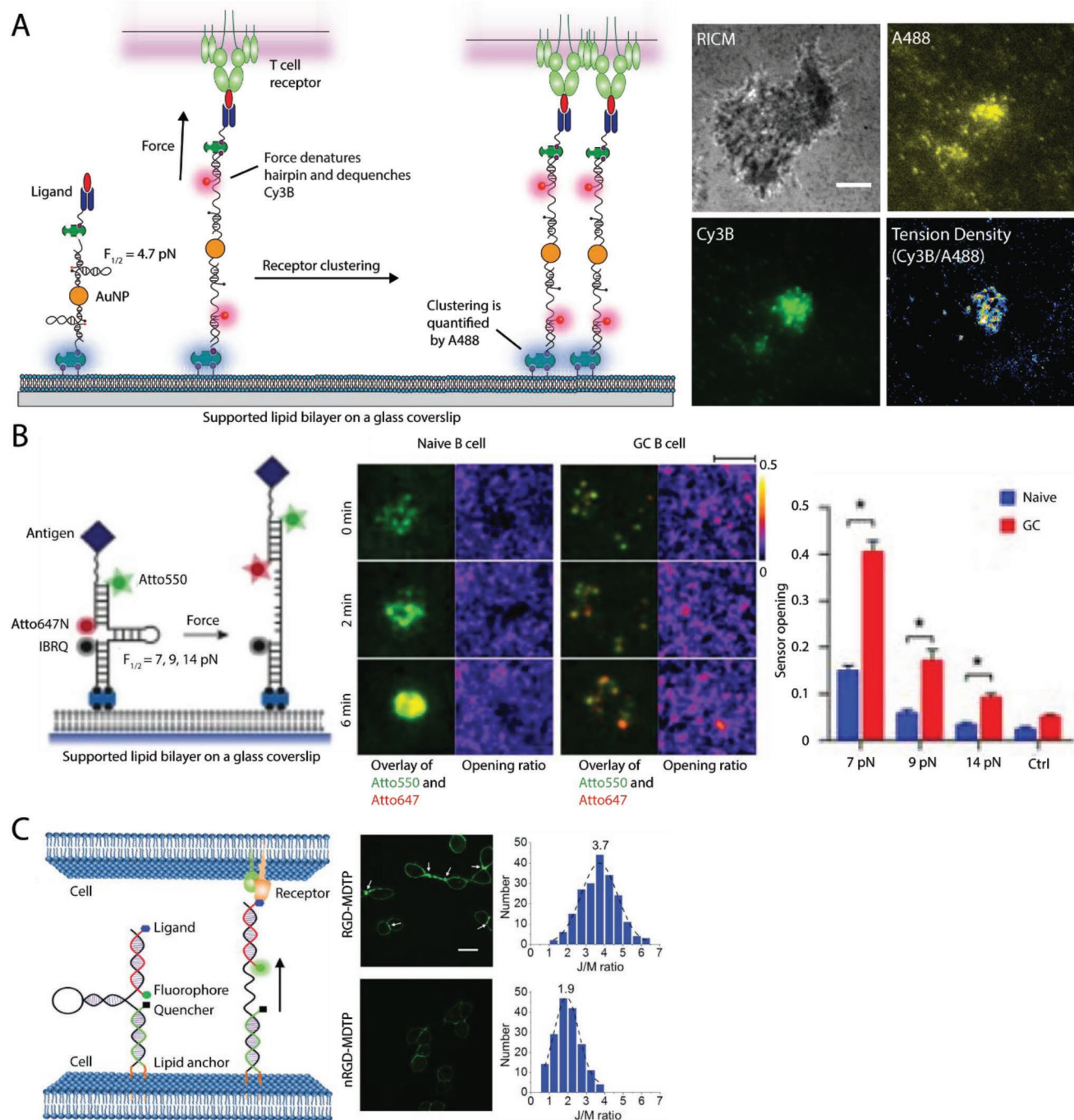
ADVANCED
SCIENCE NEWS
www.advancedsciencenews.com

NANO · MICRO
small
www.small-journal.com

Figure 10. DNA-based force probes on fluid membrane. A) Ratiometric force probes (RFPs) for mapping TCR force on a supported lipid bilayer. Clustering and force can be deconvoluted with incorporation of a second dye that is insensitive to the forces (Left). TCRs cluster RFPs at the center of cell-SLB contact and generate forces >4.7 pN to unfold the hairpin as indicated by the tension density map (right). Reproduced with permission.[71] Copyright 2016, American Chemical Society. B) A simplified version of RFP (Left). Fluorescence imaging showing the response of 9 pN RFPs at the B cell-SLB contact (middle). Bar chart showing the opening ratio of RFPs with different $F_{1/2}$ by naïve or GC B cells (Right). Reproduced with permission.[73] Copyright 2016, Springer Nature. C) DNA-based force probes anchored on a live cell to map forces involved in formation of an intracellular junction (Left). Fluorescence imaging showing clustering and probe opening at the intracellular junctions as indicated by the increase in junction/membrane fluorescence ratio (Right). Reproduced with permission.[75] Copyright 2017, American Chemical Society.

nucleic acid (PNA):DNA duplexes were found to have higher rupture forces (≈70 pN)[80] compared to its DNA:DNA counterpart by dynamic force spectroscopy measurement. It is logical to conclude that other XNAs such as threose nucleic acid (TNA), locked nucleic acid (LNA) and glycol nucleic acid (GNA) would also behave similarly.

ADVANCED
SCIENCE NEWS
www.advancedsciencenews.com

NANO · MICRO
small
www.small-journal.com

Still, directly comparing the absolute unfolding force values across different classes of DNA-based tension sensors is less meaningful when the unfolding force was determined using different methods. For example, the $F_{1/2}$ of a DNA hairpin is determined at equilibrium conditions with a constant force and this represents the minimal force to unfold a hairpin, ignoring the possibility of barriers to unfolding as the loading rate changes. More loading-rate dependent studies are needed to clearly define a relationship between loading rate and force hysteresis on the probability of DNA unfolding and refolding. However, the loading rate of receptor forces is largely unknown and likely depends on the biology of interest. Therefore, the calibrated $F_{1/2}$ for DNA-based force probes should be considered as a reference value that is related to the actual applied force.

To date, current mechanobiology studies employing DNA-based MTFM probes have aimed to measure the forces (or peak forces) transmitted by receptors leading to receptor activation. However, an emerging concept in the field is that receptors may detect and respond to the amount of mechanical work (product of force–extension) or physical extension rather than the applied force. Alternatively, receptors may be subjected to constant extension control as part of mechanosensing circuits. Key work in this area by Hoffman and co-workers has shown that a library of genetically encoded vinculin tension sensors are extended to similar levels despite experiencing different magnitudes of forces within the FA.[81] Testing these interesting concepts of whether integrins are subjected to extension-based control or work-sensing with DNA-based probes is likely to represent a future next step for the field. These concepts intimately connect with the catch-bond model which still requires validation within functional FAs in vivo.

Another challenge is the chemical stability of the DNA-based force sensors within the biological environment. Cell culture often requires media that is supplemented with significant amounts (2–20%) of serum proteins (e.g., fetal bovine serum) to support normal cell metabolism. Serum is rich in nucleases that may chemically damage the DNA force probes over time. Additionally, certain cells, when activated, secrete proteases and/or nucleases that further complicate the force measurement. For instance, we observed degradation of DNA-based force probes after incubating fibroblasts for 1–2 h, which could be due to mechanical probe shearing and nuclease digestion. Therefore, systematic investigations into the integrity of these probes over time are needed for each specific cellular model. Future work focused on developing chemically modified, nuclease resistant nucleic acids will ultimately solve this issue.

Developing new strategies to integrate these DNA-based force sensors with surfaces that have complex topography and composition could yield new insight into 2D or 3D mechanobiology. Recent work integrating DNA-based tension probes into 3D hydrogels suggests that these applications are within reach.[82] To sum, the DNA-based tension probe is rapidly transforming the study of cellular mechanotransduction. Further innovative developments will continue to push the frontiers of our capabilities as well as our fundamental understanding of molecular biophysics in developmental biology, immunology and cancer biology.

Conflict of Interest

The authors declare no conflict of interest.

[1] P. Ball, *Nature* **2013**, *494*, 32.

[2] A. Harris, P. Wild, D. Stopak, *Science* **1980**, *208*, 177.

[3] a) J. Lee, M. Leonard, T. Oliver, A. Ishihara, K. Jacobson, *J. Cell Biol.* **1994**, *127*, 1957; b) M. Dembo, Y.-L. Wang, *Biophys. J.* **1999**, *76*, 2307; c) S. A. Maskarinec, C. Franck, D. A. Tirrell, G. Ravichandran, *Proc. Natl. Acad. Sci. USA* **2009**, *106*, 22108; d) S. V. Plotnikov, B. Sabass, U. S. Schwarz, C. M. Waterman, in *Methods in Cell Biology*, Vol. *123* (Eds: J. C. Waters, T. Wittman), Elsevier, Atlanta, GA **2014**, pp. 367; e) R. W. Style, R. Boltyanskiy, G. K. German, C. Hyland, C. W. MacMinn, A. F. Mertz, L. A. Wilen, Y. Xu, E. R. Dufresne, *Soft Matter* **2014**, *10*, 4047.

[4] a) J. L. Tan, J. Tien, D. M. Pirone, D. S. Gray, K. Bhadriraju, C. S. Chen, *Proc. Natl. Acad. Sci. USA* **2003**, *100*, 1484; b) J. Fu, Y.-K. Wang, M. T. Yang, R. A. Desai, X. Yu, Z. Liu, C. S. Chen, *Nat. Methods* **2010**, *7*, 733; c) S. Ghassemi, G. Meacci, S. Liu, A. A. Gondarenko, A. Mathur, P. Roca-Cusachs, M. P. Sheetz, J. Hone, *Proc. Natl. Acad. Sci. USA* **2012**, *109*, 5328.

[5] K. C. Neuman, A. Nagy, *Nat. Methods* **2008**, *5*, 491.

[6] A. Fuhrmann, R. Ros, *Nanomedicine* **2010**, *5*, 657.

[7] a) K. Haase, A. E. Pelling, *J. R. Soc., Interface* **2015**, *12*, 20140970; b) N. Gavara, *Microsc. Res. Tech.* **2017**, *80*, 75.

[8] D. R. Stabley, C. Jurchenko, S. S. Marshall, K. S. Salaita, *Nat. Methods* **2012**, *9*, 64.

[9] a) Y. Liu, K. Yehl, Y. Narui, K. Salaita, *J. Am. Chem. Soc.* **2013**, *135*, 5320; b) Y. Liu, R. Medda, Z. Liu, K. Galior, K. Yehl, J. P. Spatz, E. A. Cavalcanti-Adam, K. Salaita, *Nano Lett.* **2014**, *14*, 5539; c) Y. Chang, Z. Liu, Y. Zhang, K. Galior, J. Yang, K. Salaita, *J. Am. Chem. Soc.* **2016**, *138*, 2901.

[10] Y. Zhang, C. Ge, C. Zhu, K. Salaita, *Nat. Commun.* **2014**, *5*, 5167.

[11] M. Morimatsu, A. H. Mekhdjian, A. C. Chang, S. J. Tan, A. R. Dunn, *Nano Lett.* **2015**, *15*, 2220.

[12] a) K. Galior, Y. Liu, K. Yehl, S. Vivek, K. Salaita, *Nano Lett.* **2016**, *16*, 341; b) K. Galior, V. P.-Y. Ma, Y. Liu, H. Su, N. Baker, R. A. Panettieri Jr., C. Wongtrakool, K. Salaita, *Adv. Healthcare Mater.* **2018**, *7*, 1800069.

[13] a) C. Jurchenko, K. S. Salaita, *Mol. Cell. Biol.* **2015**, *35*, 2570; b) Y. Liu, K. Galior, V. P.-Y. Ma, K. Salaita, *Acc. Chem. Res.* **2017**, *50*, 2915.

ADVANCED
SCIENCE NEWS
www.advancedsciencenews.com

NANO · MICRO
small
www.small-journal.com

[14] N. C. Seeman, *J. Theor. Biol.* **1982**, *99*, 237.

[15] M. R. Jones, N. C. Seeman, C. A. Mirkin, *Science* **2015**, *347*, 1260901.

[16] a) A. D. Ellington, J. W. Szostak, *Nature* **1990**, *346*, 818; b) C. Tuerk, L. Gold, *Science* **1990**, *249*, 505.

[17] E. J. Cho, J.-W. Lee, A. D. Ellington, *Annu. Rev. Anal. Chem.* **2009**, *2*, 241.

[18] a) R. R. Breaker, G. F. Joyce, *Chem. Biol.* **1994**, *1*, 223; b) R. R. Breaker, *Nat. Biotechnol.* **1997**, *15*, 427; c) S. K. Silverman, *Trends Biochem. Sci.* **2016**, *41*, 595.

[19] a) D. Nykypanchuk, M. M. Maye, D. van der Lelie, O. Gang, *Nature* **2008**, *451*, 549; b) S. Y. Park, A. K. R. Lytton-Jean, B. Lee, S. Weigand, G. C. Schatz, C. A. Mirkin, *Nature* **2008**, *451*, 553; c) R. J. Macfarlane, B. Lee, M. R. Jones, N. Harris, G. C. Schatz, C. A. Mirkin, *Science* **2011**, *334*, 204.

[20] a) T.-G. Cha, J. Pan, H. Chen, J. Salgado, X. Li, C. Mao, J. H. Choi, *Nat. Nanotechnol.* **2014**, *9*, 39; b) K. Yehl, A. Mugler, S. Vivek, Y. Liu, Y. Zhang, M. Fan, E. R. Weeks, K. Salaita, *Nat. Nanotechnol.* **2016**, *11*, 184; c) K. M. Cherry, L. Qian, *Nature* **2018**, *559*, 370.

[21] a) C. R. Dass, P. F. M. Choong, L. M. Khachigian, *Mol. Cancer Ther.* **2008**, *7*, 243; b) K. Yehl, J. P. Joshi, B. L. Greene, R. B. Dyer, R. Nahta, K. Salaita, *ACS Nano* **2012**, *6*, 9150; c) I. Somasuntharam, K. Yehl, S. L. Carroll, J. T. Maxwell, M. D. Martinez, P.-L. Che, M. E. Brown, K. Salaita, M. E. Davis, *Biomaterials* **2016**, *83*, 12; d) H. Fan, X. Zhang, Y. Lu, *Sci. China: Chem.* **2017**, *60*, 591; e) J. R. Petree, K. Yehl, K. Galior, R. Glazier, B. Deal, K. Salaita, *ACS Chem. Biol.* **2018**, *13*, 215.

[22] a) D.-L. Ma, V. P.-Y. Ma, D. S.-H. Chan, K.-H. Leung, H.-Z. He, C.-H. Leung, *Coord. Chem. Rev.* **2012**, *256*, 3087; b) S.-F. Torabi, Y. Lu, *Curr. Opin. Biotechnol.* **2014**, *28*, 88; c) W. Zhou, R. Saran, J. Liu, *Chem. Rev.* **2017**, *117*, 8272.

[23] a) C. Albrecht, K. Blank, M. Lalic-Mülthaler, S. Hirler, T. Mai, I. Gilbert, S. Schiffmann, T. Bayer, H. Clausen-Schaumann, H. E. Gaub, *Science* **2003**, *301*, 367; b) D. Ho, K. Falter, P. Severin, H. E. Gaub, *Anal. Chem.* **2009**, *81*, 3159; c) K. Limmer, D. A. Pippig, D. Aschenbrenner, H. E. Gaub, *PLoS One* **2014**, *9*, e89626.

[24] a) H. Lin, L. Sun, R. M. Crooks, *J. Am. Chem. Soc.* **2005**, *127*, 11210; b) H. Lin, J. Kim, L. Sun, R. M. Crooks, *J. Am. Chem. Soc.* **2006**, *128*, 3268.

[25] C. Bustamante, Y. R. Chemla, N. R. Forde, D. Izhaky, *Annu. Rev. Biochem.* **2004**, *73*, 705.

[26] A. Tajik, Y. Zhang, F. Wei, J. Sun, Q. Jia, W. Zhou, R. Singh, N. Khanna, A. S. Belmont, N. Wang, *Nat. Mater.* **2016**, *15*, 1287.

[27] J.-B. Lee, R. K. Hite, S. M. Hamdan, X. Sunney Xie, C. C. Richardson, A. M. van Oijen, *Nature* **2006**, *439*, 621.

[28] J.-C. Liao, Y.-J. Jeong, D.-E. Kim, S. S. Patel, G. Oster, *J. Mol. Biol.* **2005**, *350*, 452.

[29] a) H.-Y. Wang, T. Elston, A. Mogilner, G. Oster, *Biophys. J.* **1998**, *74*, 1186; b) J. Chen, S. Le, A. Basu, W. J. Chazin, J. Yan, *Sci. Rep.* **2015**, *5*, 9296.

[30] a) K. Neupane, D. A. N. Foster, D. R. Dee, H. Yu, F. Wang, M. T. Woodside, *Science* **2016**, *352*, 239; b) H. Yu, M. G. W. Siewny, D. T. Edwards, A. W. Sanders, T. T. Perkins, *Science* **2017**, *355*, 945.

[31] F. Rico, A. Russek, L. González, H. Grubmüller, S. Scheuring, *Proc. Natl. Acad. Sci. USA* **2019**, *116*, 6594.

[32] G. Bell, *Science* **1978**, *200*, 618.

[33] S. Guo, Q. Tang, M. Yao, H. You, S. Le, H. Chen, J. Yan, *Chem. Sci.* **2018**, *9*, 5871.

[34] R. Krautbauer, M. Rief, H. E. Gaub, *Nano Lett.* **2003**, *3*, 493.

[35] S. Hohng, R. Zhou, M. K. Nahas, J. Yu, K. Schulten, D. M. J. Lilley, T. Ha, *Science* **2007**, *318*, 279.

[36] M. T. Woodside, W. M. Behnke-Parks, K. Larizadeh, K. Travers, D. Herschlag, S. M. Block, *Proc. Natl. Acad. Sci. USA* **2006**, *103*, 6190.

[37] K. Hatch, C. Danilowicz, V. Coljee, M. Prentiss, *Phys. Rev. E* **2008**, *78*, 011920.

[38] J. Zhang, Y. Yan, S. Samai, D. S. Ginger, *J. Phys. Chem. B* **2016**, *120*, 10706.

[39] a) T. Strunz, K. Oroszlan, R. Schäfer, H.-J. Güntherodt, *Proc. Natl. Acad. Sci. USA* **1999**, *96*, 11277; b) S. Cocco, R. Monasson, J. F. Marko, *Proc. Natl. Acad. Sci. USA* **2001**, *98*, 8608; c) P.-G. de Gennes, *C.R. Acad. Sci., Ser. V: Phys.* **2001**, *2*, 1505; d) A. R. Singh, D. Giri, S. Kumar, *J. Chem. Phys.* **2010**, *132*, 235105; e) M. Mosayebi, A. A. Louis, J. P. K. Doye, T. E. Ouldridge, *ACS Nano* **2015**, *9*, 11993.

[40] X. Wang, T. Ha, *Science* **2013**, *340*, 991.

[41] Y. Murad, I. T. S. Li, *Biophys. J.* **2019**, *116*, 1282.

[42] a) A. C. Chang, A. H. Mekhdjian, M. Morimatsu, A. K. Denisin, B. L. Pruitt, A. R. Dunn, *ACS Nano* **2016**, *10*, 10745; b) S. J. Tan, A. C. Chang, C. M. Miller, S. M. Anderson, L. S. Prahl, D. J. Odde, A. R. Dunn, *bioRxiv* **2019**, 530469.

[43] W. J. Galush, J. A. Nye, J. T. Groves, *Biophys. J.* **2008**, *95*, 2512.

[44] Y. Zhang, Y. Qiu, A. T. Blanchard, Y. Chang, J. M. Brockman, V. P.-Y. Ma, W. A. Lam, K. Salaita, *Proc. Natl. Acad. Sci. USA* **2018**, *115*, 325.

[45] a) S. Schwarz Henriques, R. Sandmann, A. Strate, S. Köster, *J. Cell Sci.* **2012**, *125*, 3914; b) J. Hanke, D. Probst, A. Zemel, U. S. Schwarz, S. Köster, *Soft Matter* **2018**, *14*, 6571.

[46] Y. Liu, L. Blanchfield, V. P.-Y. Ma, R. Andargachew, K. Galior, Z. Liu, B. Evavold, K. Salaita, *Proc. Natl. Acad. Sci. USA* **2016**, *113*, 5610.

[47] M. Grandbois, M. Beyer, M. Rief, H. Clausen-Schaumann, H. E. Gaub, *Science* **1999**, *283*, 1727.

[48] C. S. Yun, A. Javier, T. Jennings, M. Fisher, S. Hira, S. Peterson, B. Hopkins, N. O. Reich, G. F. Strouse, *J. Am. Chem. Soc.* **2005**, *127*, 3115.

[49] J. Hong, C. Ge, P. Jothikumar, Z. Yuan, B. Liu, K. Bai, K. Li, W. Rittase, M. Shinzawa, Y. Zhang, A. Palin, P. Love, X. Yu, K. Salaita, B. D. Evavold, A. Singer, C. Zhu, *Nat. Immunol.* **2018**, *19*, 1379.

[50] B. L. Blakely, C. E. Dumelin, B. Trappmann, L. M. McGregor, C. K. Choi, P. C. Anthony, V. K. Duesterberg, B. M. Baker, S. M. Block, D. R. Liu, C. S. Chen, *Nat. Methods* **2014**, *11*, 1229.

[51] X. Wang, Z. Rahil, I. T. S. Li, F. Chowdhury, D. E. Leckband, Y. R. Chemla, T. Ha, *Sci. Rep.* **2016**, *6*, 21584.

[52] S. Anwesha, Z. Yuanchang, W. Yongliang, W. Xuefeng, *Phys. Biol.* **2018**, *15*, 065002.

[53] Y. Wang, X. Wang, *Sci. Rep.* **2016**, *6*, 36959.

[54] F. Chowdhury, I. T. S. Li, T. T. M. Ngo, B. J. Leslie, B. C. Kim, J. E. Sokoloski, E. Weiland, X. Wang, Y. R. Chemla, T. M. Lohman, T. Ha, *Nano Lett.* **2016**, *16*, 3892.

[55] V. C. Luca, B. C. Kim, C. Ge, S. Kakuda, D. Wu, M. Roein-Peikar, R. S. Haltiwanger, C. Zhu, T. Ha, K. C. Garcia, *Science* **2017**, *355*, 1320.

[56] I. T. S. Li, T. Ha, Y. R. Chemla, *Sci. Rep.* **2017**, *7*, 44502.

[57] M. H. Jo, W. T. Cottle, T. Ha, *ACS Biomater. Sci. Eng.* **2018**, *4*, 4278.

[58] Y. Wang, D. N. LeVine, M. Gannon, Y. Zhao, A. Sarkar, B. Hoch, X. Wang, *Biosens. Bioelectron.* **2018**, *100*, 192.

[59] Y. Zhao, Y. Wang, A. Sarkar, X. Wang, *iScience* **2018**, *9*, 502.

[60] V. P.-Y. Ma, Y. Liu, K. Yehl, K. Galior, Y. Zhang, K. Salaita, *Angew. Chem., Int. Ed.* **2016**, *55*, 5488.

[61] J. M. Brockman, A. T. Blanchard, V. Pui-Yan Ma, W. D. Derricotte, Y. Zhang, M. E. Fay, W. A. Lam, F. A. Evangelista, A. L. Mattheyses, K. Salaita, *Nat. Methods* **2018**, *15*, 115.

[62] a) F. Hong, F. Zhang, Y. Liu, H. Yan, *Chem. Rev.* **2017**, *117*, 12584; b) P. Wang, T. A. Meyer, V. Pan, P. K. Dutta, Y. Ke, *Chem* **2017**, *2*, 359.

[63] A. Shaw, V. Lundin, E. Petrova, F. Fördős, E. Benson, A. Al-Amin, A. Herland, A. Blokzijl, B. Högberg, A. I. Teixeira, *Nat. Methods* **2014**, *11*, 841.

1900961 (17 of 18)

[64] P. K. Dutta, Y. Zhang, A. T. Blanchard, C. Ge, M. Rushdi, K. Weiss, C. Zhu, Y. Ke, K. Salaita, *Nano Lett.* **2018**, *18*, 4803.

[65] B. N. Manz, J. T. Groves, *Nat. Rev. Mol. Cell Biol.* **2010**, *11*, 342.

[66] L. K. Tamm, H. M. McConnell, *Biophys. J.* **1985**, *47*, 105.

[67] Y.-H. M. Chan, S. G. Boxer, *Curr. Opin. Chem. Biol.* **2007**, *11*, 581.

[68] a) E. T. Castellana, P. S. Cremer, *Surf. Sci. Rep.* **2006**, *61*, 429; b) K. L. Hartman, S. Kim, K. Kim, J.-M. Nam, *Nanoscale* **2015**, *7*, 66.

[69] R. Glazier, K. Salaita, *Biochim. Biophys. Acta, Biomembr.* **2017**, *1859*, 1465.

[70] a) A. Grakoui, S. K. Bromley, C. Sumen, M. M. Davis, A. S. Shaw, P. M. Allen, M. L. Dustin, *Science* **1999**, *285*, 221; b) S. K. Bromley, W. R. Burack, K. G. Johnson, K. Somersalo, T. N. Sims, C. Sumen, M. M. Davis, A. S. Shaw, P. M. Allen, M. L. Dustin, *Annu. Rev. Immunol.* **2001**, *19*, 375.

[71] V. P.-Y. Ma, Y. Liu, L. Blanchfield, H. Su, B. D. Evavold, K. Salaita, *Nano Lett.* **2016**, *16*, 4552.

[72] E. Natkanski, W.-Y. Lee, B. Mistry, A. Casal, J. E. Molloy, P. Tolar, *Science* **2013**, *340*, 1587.

[73] C. R. Nowosad, K. M. Spillane, P. Tolar, *Nat. Immunol.* **2016**, *17*, 870.

[74] K. Kwak, N. Quizon, H. Sohn, A. Saniee, J. Manzella-Lapeira, P. Holla, J. Brzostowski, J. Lu, H. Xie, C. Xu, K. M. Spillane, P. Tolar, S. K. Pierce, *Sci. Immunol.* **2018**, *3*, eaau6598.

[75] B. Zhao, C. O'Brien, A. P. K. K. K. Mudiyanselage, N. Li, Y. Bagheri, R. Wu, Y. Sun, M. You, *J. Am. Chem. Soc.* **2017**, *139*, 18182.

[76] W. Becker, *J.Microsc.* **2012**, *247*, 119.

[77] a) Z. Yu, J. D. Schonhoft, S. Dhakal, R. Bajracharya, R. Hegde, S. Basu, H. Mao, *J. Am. Chem. Soc.* **2009**, *131*, 1876; b) Y. Cheng, Q. Tang, Y. Li, Y. Zhang, C. Zhao, J. Yan, H. You, *J. Biol. Chem.* **2019**, *294*,5890.

[78] S. Dhakal, J. D. Schonhoft, D. Koirala, Z. Yu, S. Basu, H. Mao, *J. Am. Chem. Soc.* **2010**, *132*, 8991.

[79] D. Koirala, P. Shrestha, W. J. Maximuck, Y. Cui, H. Mao, K. Hidaka, T. Emura, H. Sugiyama, M. Endo, *Nucleic Acids Res.* **2016**, *44*, 6574.

[80] a) H. Zohar, C. L. Hetherington, C. Bustamante, S. J. Muller, *Nano Lett.* **2010**, *10*, 4697; b) S. Dutta, B. A. Armitage, Y. L. Lyubchenko, *Biochemistry* **2016**, *55*, 1523.

[81] A. S. LaCroix, A. D. Lynch, M. E. Berginski, B. D. Hoffman, *eLife* **2018**, *7*, e33927.

[82] R. Merindol, G. Delechiave, L. Heinen, L. H. Catalani, A. Walther, *Nat. Commun.* **2019**, *10*, 528.